iScience

CellPress
OPEN ACCESS

Article

Residue-Specific Message Encoding in CD40-Ligand

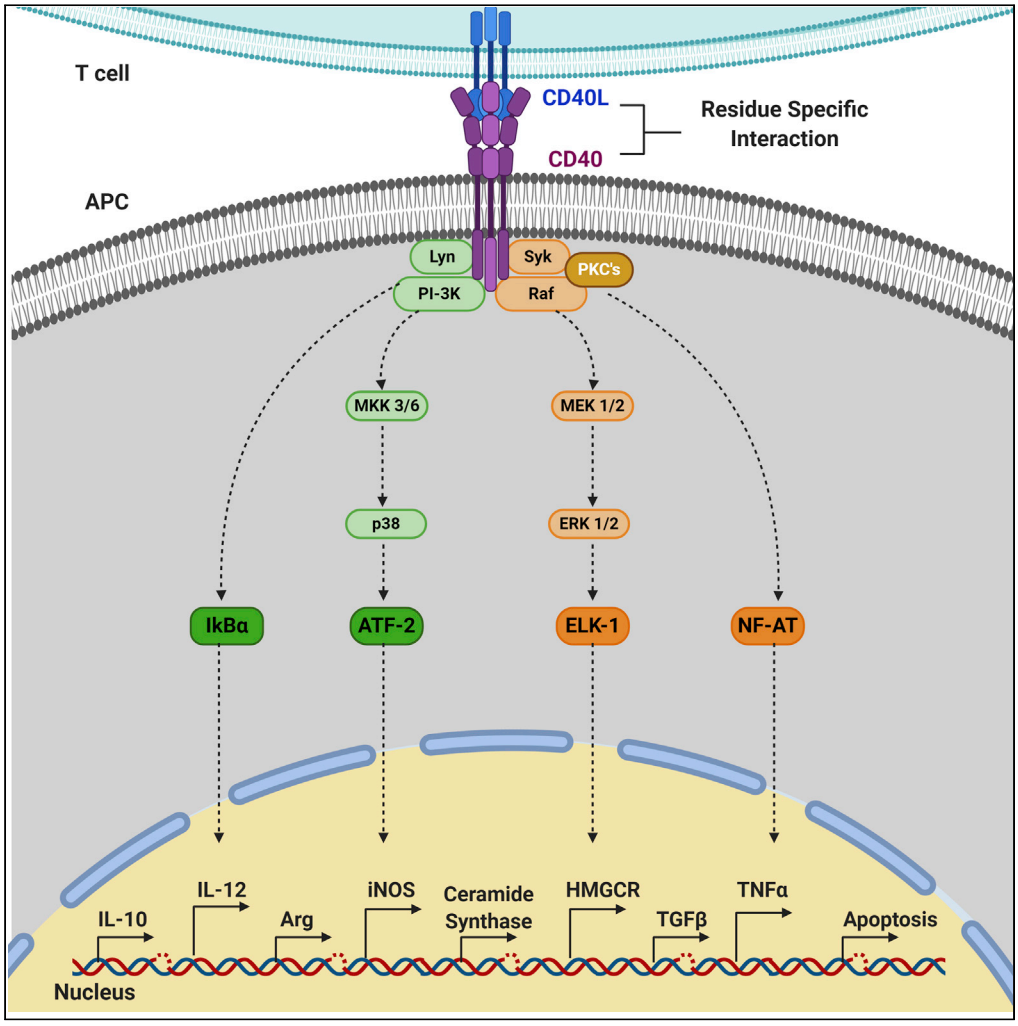

Aditya Yashwant Sarode, Mukesh Kumar Jha, Shubhranshu Zutshi, Soumya Kanti Ghosh, Hima Mahor, Uddipan Sarma, Bhaskar Saha

sarode.aditya@gmail.com, sarodeaditya@yahoo.com (A.Y.S.) bhaskar211964@yahoo.com, saha.bhaskar12345@gmail.com (B.S.)

HIGHLIGHTS

Contact residues on CD40L, when mutated to Valine, alter signaling specificity

The specificity is dictated by Residue-specific CD40L-CD40 interaction

Cytokine release, apoptosis, antileishmanial activity imply functional specificity

Specific CD40-CD40L interaction for antileishmanial functions in BALB/c mice

Sarode et al., iScience *23*, 101441
September 25, 2020
https://doi.org/10.1016/j.isci.2020.101441

iScience

CellPress
OPEN ACCESS

Article

Residue-Specific Message Encoding in CD40-Ligand

Aditya Yashwant Sarode,[1,3,*] Mukesh Kumar Jha,[1] Shubhranshu Zutshi,[1] Soumya Kanti Ghosh,[1] Hima Mahor,[1] Uddipan Sarma,[1] and Bhaskar Saha[1,2,3,*]

SUMMARY

CD40-Ligand (CD40L)-CD40 interaction regulates immune responses against pathogens, autoantigens, and tumor and transplantation antigens. Single amino acid mutations within the 115–155 amino acids stretch, which is responsible for CD40L functions, result in XIgM syndrome. We hypothesize that each of these amino acids of CD40L encodes specific message that, when decoded by CD40 signaling, induces a specific profile of functions. We observed that every single substitution in the XIgM-related amino acids in the 115–155 41-mer peptide in CD40L selectively altered CD40 signaling and effector functions—cytokine productions, HMGCoA reductase, ceramide synthase, inducible nitric oxide synthase and arginase expression, survival of B cells, and control of *Leishmania* infection and anti-leishmanial T cell response—suggesting residue-specific encoding of a distinct set of messages that collectively define CD40L pleiotropy, serve as a target for engineering the ligand to generate superagonists as immunotherapeutic, and implicate the evolutionary diversification of functions among the ligands in a protein superfamily.

INTRODUCTION

CD40L-CD40 interaction, one of the crucial interfaces between the innate and adaptive responses, plays a decisive role in modulating cytokines and consequential effector T cells in pathogenic responses, germinal center formation, affinity maturation, survival, proliferation, memory, autoimmunity, cancer, transplantations, and atherosclerosis (van Kooten and Banchereau, 2000; Reichmann et al., 2000; Murugaiyan et al., 2007; Kumanogoh et al., 2001). CD40L binding of CD40 results in multiple signaling events that lead to pleiotropic functions. The receptor CD40 lacks the kinase domain; it recruits TNF-α Receptor Associated Factors (TRAFs) at the cytoplasmic domain upon activation (Schröfelbauer and Hoffmann, 2011; Laporte et al., 2008). The TRAFs activate the signaling pathways like Phosphatidylinositol 3-phosphate (PI3K), Raf, Lyn, Syk, p38, ERK, and Protein Kinase C (PKCs). Both TRAF-dependent and -independent signaling activate these signaling intermediates. CD40 signaling leads to activation of both canonical and non-canonical NF-κB pathways and of other associated Transcription Factors (TFs) such as ATF2, ELK1, BLIMP-1, BATF, and NFAT initiating differential gene expression and the ensuing effector function (Elgueta et al., 2009; Elgueta et al., 2010; Roy et al., 2015; Busch et al., 2016). CD40L-CD40 signaling is exploited by many pathogens for their survival; the switching of CD40 signaling to heighten the production of anti-inflammatory cytokines is a clear example (Mathur et al., 2004). During leishmanial infection, CD40 signaling is skewed toward the anti-inflammatory pathways involving cRaf, Syk, MEK1/2, ERK1/2, PKCδ, and PKCζ. However, stimulation with CD40L results in the skewing of the signaling toward pro-inflammatory pathway involving Lyn, PI3K, MKK3/6, p38, PKCα, and PKCβII (Awasthi et al., 2003; Khan et al., 2012, 2014; Mathur et al., 2004; Murugaiyan et al., 2006; Rub et al., 2009; Sudan et al., 2012). In addition, it was shown that LMP-1, a protein encoded by Epstein-Barr virus signaling like CD40, rescued certain functions—but not the full range—associated with the CD40 in $CD40^{-/-}$ mice suggesting that there existed CD40L residue-specific signaling and functions (Uchida et al., 1999). Given the broad spectrum of signaling molecules activated by CD40 and its duality in pro- and anti-inflammatory responses, the origin of the specificity remains undetermined. Moreover, the cooperation and dissension between various signaling molecules in triggering gene expression and associated functions still remain to be uncovered. Therefore, it would be substantial in understanding the specific role of individual residues present on CD154 during the CD40 signaling and dissecting out the contribution in each pathway to carry out the effector function.

[1]National Centre for Cell Science, Lab-5, Pathogenesis and Cellular Response, Ganeshkhind, Pune, Maharashtra 411007, India

[2]Trident Academy of Creative Technology, Bhubaneswar, Orissa 751024, India

[3]Lead Contact

*Correspondence: sarode.aditya@gmail.com, sarodeaditya@yahoo.com (A.Y.S.), bhaskar211964@yahoo.com, saha.bhaskar12345@gmail.com (B.S.)

https://doi.org/10.1016/j.isci.2020.101441

The complementarity-guided co-evolution of ligand-receptor systems often resulted in super-families of related ligands, implying the amino acid residue-specific interactions and continuous gain or loss of functions that relate to the evolutionary fitness (Siddiq et al., 2017; Root-Bernstein, 2005; Starr and Thornton, 2016; Di Roberto et al., 2017; Thornton, 2001; Spangler et al., 2015). As mutation is a random process, any mutation that could lead to the loss of receptor binding and function were preferentially eliminated, keeping only those that favor the binding and specific function. CD40L mutations are associated with XIgM syndrome characterized by impaired B cells immunoglobulin class switching and recurrent infections of the affected individuals (Seyama et al., 1998; Macchi et al., 1995; Yamniuk et al., 2016). Although some of the CD40L mutations (deletion or nonsense) lead to truncated protein or improper folding to result in the loss of surface expression, there are point mutations that allow proper folding and surface expression of the CD40L but induce subtle yet substantial conformational changes to impede the CD40 signals. Reports suggest that the 115–155 amino acids stretch of CD40L is involved in the binding of the CD40 and are hotspots for mutations reported in XIgM (Yamniuk et al., 2016; Bajorath, 1998; Bajorath et al., 1995, 1996). Structural studies using bioinformatics tools and homology modeling revealed certain amino acids more critical during the interaction involving charged complementarities between the interacting residues in addition to hydrogen bonding. These included K133, E142, and K143, which has a direct role to pay in binding with CD40 and are charged. Moreover E129, K143, G144, Y145, and Y146 have a role in hydrophilic interaction with CD40 residues, whereas residue A130 has a hydrophobic interaction with CD40 receptor. Such interactions at this region (S128 to K149) are reported to be mutated in XIgM syndrome and are therefore implied in triggering CD40 signaling and effector functions (Thusberg and Vihinen, 2007; Karpusas et al., 2001; Garber et al., 1999; An et al., 2011).

As any of these mutations in XIgM led to similar deficiency in B cell function, the residue-specific message encoding in a ligand could not be envisaged. In order to decipher the specific messages encoded in each of these residues in the CD40L, we mutated each of these XIgM-implicated residues to valine and studied the changes in CD40 signaling and functions as compared with those triggered by wild-type CD40L. The profile of changes in all the assessed functions together defines the message encoded by the mutated amino acid. Herein, using CD40-CD40L as a model receptor-ligand system, we thus examine the residue-specific assignment of functions that also relate to the ligand-encoded messages that are transferred to the receptor during the receptor-ligand interaction.

RESULTS

The Point Substitutions Do Not Affect the Secondary Structures of the 41-mer Peptides

Originally discovered through B cell activation and survival,CD40-CD40L interaction was subsequently implicated in XIgM syndrome, characterized by hyper-IgM production and mutations in the CD40L 127–148 amino acid stretch (Bajorath et al., 1995, 1996; Bajorath, 1998; An et al., 2011). As any of these mutations led to similar deficiency in B cell function, the idea of residue-specific function was never conceived. In order to decipher the specific messages encoded in each of these residues in the CD40L, we synthesized the 41-mer peptides (115–155 amino acids)—strongly homologous sequence between mice and humans (Figure S1)—with single XIgM-related amino acid substitutions to Valine and assessed their functions in mouse macrophages and their anti-leishmanial functions in susceptible BALB/c mice. Structure of 41-mer peptide was predicted using iTASSAR (Roy et al., 2010) and is displayed as corresponding part of whole CD40L (Figure 1A). These substitutions, except in peptide 10, did not introduce any instability to the secondary structural differences as compared with the secondary structure of the wild-type (Figures 1B and 1C).

Mutant Peptides Can Initiate Multiple Signaling Cascades

We first assessed the CD40 signaling, as previously worked out (Mathur et al., 2004; Sudan et al., 2012; Martin et al., 2010; Awasthi et al., 2003), triggered by the wild-type and mutant CD40L peptides. We observed that, compared with the wild-type peptide, the peptides 7 and 8 induced higher p38MAPK, Lyn, PKCβII, and PKCα phosphorylation, whereas peptides 7, 9, and 10 induced higher PI3K phosphorylation. Peptide 7 induced higher MKK3/6 phosphorylation than that induced by the wild-type peptide (Figures 2A–2D, and S2A–S2D). By contrast, ERK1/2, MEK1/2, Syk, and PKCζ phosphorylation was less induced by the peptides 7 and 8 than that induced by the wild-type. Mutant 5 induced higher MKK3/6 and cRaf, but less PKCβII, phosphorylation than that observed with the wild-type. Peptides 2, 3, 4, and 5 were least active in phosphorylating Lyn, Syk, PI3K, PKCα, PKCβII, PKCζ, MEK1/2, p38MAPK, and ERK1/2 (Figures 2A–2D and S2A–S2D). The profile of collective signaling changes with each amino acid substitution thus identifying the signals associated with that particular residue in the wild-type.

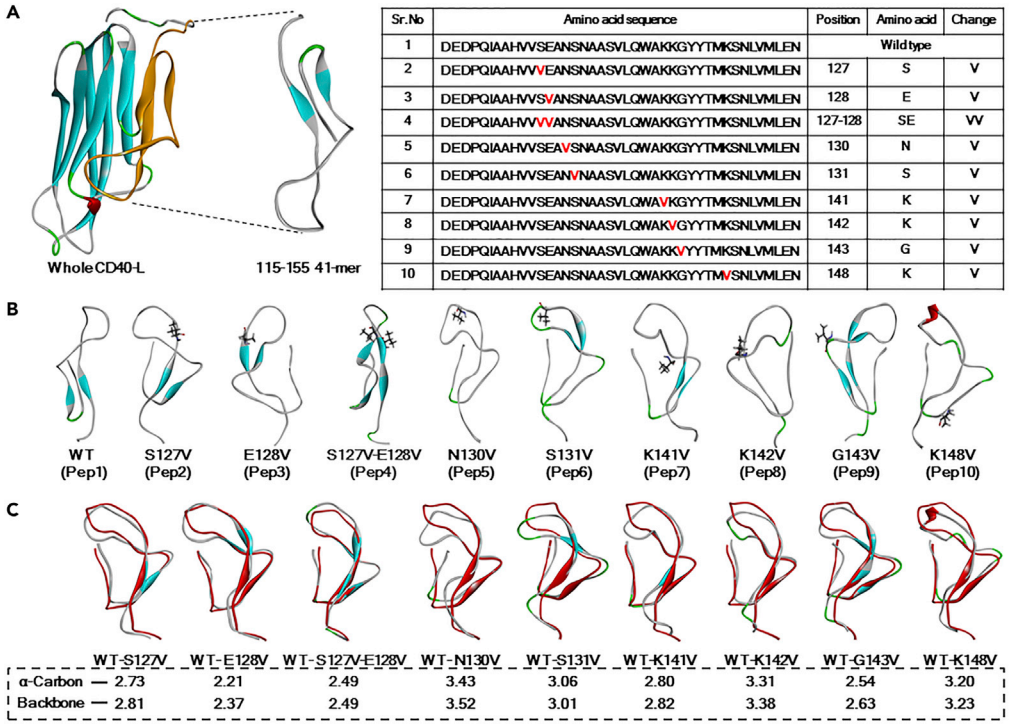

Sr.No	Amino acid sequence	Position	Amino acid	Change
1	DEDPQIAAHVVSEANSNAASVLQWAKKGYYTMKSNLVMLEN	Wild type		
2	DEDPQIAAHVV**V**EANSNAASVLQWAKKGYYTMKSNLVMLEN	127	S	V
3	DEDPQIAAHVVS**V**ANSNAASVLQWAKKGYYTMKSNLVMLEN	128	E	V
4	DEDPQIAAHVV**VV**ANSNAASVLQWAKKGYYTMKSNLVMLEN	127-128	SE	VV
5	DEDPQIAAHVVSEA**V**SNAASVLQWAKKGYYTMKSNLVMLEN	130	N	V
6	DEDPQIAAHVVSEAN**V**NAASVLQWAKKGYYTMKSNLVMLEN	131	S	V
7	DEDPQIAAHVVSEANSNAASVLQWA**V**KGYYTMKSNLVMLEN	141	K	V
8	DEDPQIAAHVVSEANSNAASVLQWAK**V**GYYTMKSNLVMLEN	142	K	V
9	DEDPQIAAHVVSEANSNAASVLQWAKK**V**YYTMKSNLVMLEN	143	G	V
10	DEDPQIAAHVVSEANSNAASVLQWAKKGYYTM**V**SNLVMLEN	148	K	V

Figure 1. Details of Mutated Peptides and Their Position on the Protein Structure

(A) Secondary structure of 41-mer CD40L and its position in the whole mouse CD40-ligand and the table mentioning the mutated amino acids (in red color) in the peptide chain.

(B) The stick representation of the mutated residues on the 41-mer I-Tasser predicted peptide structures.

(C) The variation in the structure conformation of each mutated peptide compared with the wild-type peptide by Superpose (wild-type peptide colored Red; mutated peptides have secondary structure color representation). The inset shows the root-mean-square deviation (RMSD) in the secondary structure of α-Carbon and the protein backbone in each mutated peptide compared with the wild-type peptide structure. The RMSD values are denoted with Å (Angstrom unit). See also Figure S1.

Because the signals through kinases converge on the transcription factors that carry the message to the nucleus for effecting gene transcription and effector functions (Busch et al., 2016; Baccam et al., 2003; Liao et al., 2011; Roy et al., 2015; Severa et al., 2014; Suttles et al., 1999), we assessed the phosphorylation of key transcription factors in CD40 signaling. Peptides 7 and 8 showed the highest phosphorylation of IκBα, which upon phosphorylation relieves NF-κB to be activated by phosphorylation. Peptides 2, 5, and 10 activated IκBα to a lesser extent, whereas peptides 3, 4, and 9 could not activate IκBα. Peptides 7, 8, and 9 showed the highest ATF2 and ELK1 phosphorylation, whereas the other peptides activated only ELK1 but down-regulated ATF2. Peptide 8 activated NFAT the most, whereas peptides 4 and 5 activated NFAT the least (Figures 2E and S2E). Such specificities in the activation of BATF, an AP1 family transcription factor, and BLIMP-1, a zinc finger protein transcription factor, were observed with these peptides (Figures 3A and 3B). It was observed that the expression of BATF was increased in the cells treated with the peptides 6 and 8, whereas rest of the peptides showed reduced expression. BLIMP-1 expression was highest in the cells pre-treated with peptides 5, 4, 2, and 3, whereas it was unchanged for peptide number 9 in comparison with the wild-type peptide. As summarized, the profiles of alterations in the signaling intermediates' and transcription factors' activation assign specificities to each of the substituted amino acids (Figure 2F).

Mutant Peptides Differentially Regulate PD-L1 Expression Modulating Cell Survival

In order to comprehend functional consequence of the differential activation of signaling molecules, imparted owing to the peptides, we checked the expression of PD-L1 on $CD11b^{+}$ macrophages. We could observe that the expression of PD-L1 was reduced in the macrophages that were treated with peptide 7 followed by peptide 8 and 6, whereas it was unchanged for the rest of the peptide stimulations. Since the production of different cytokines during the APC-T cell interaction has a range of outcome on the

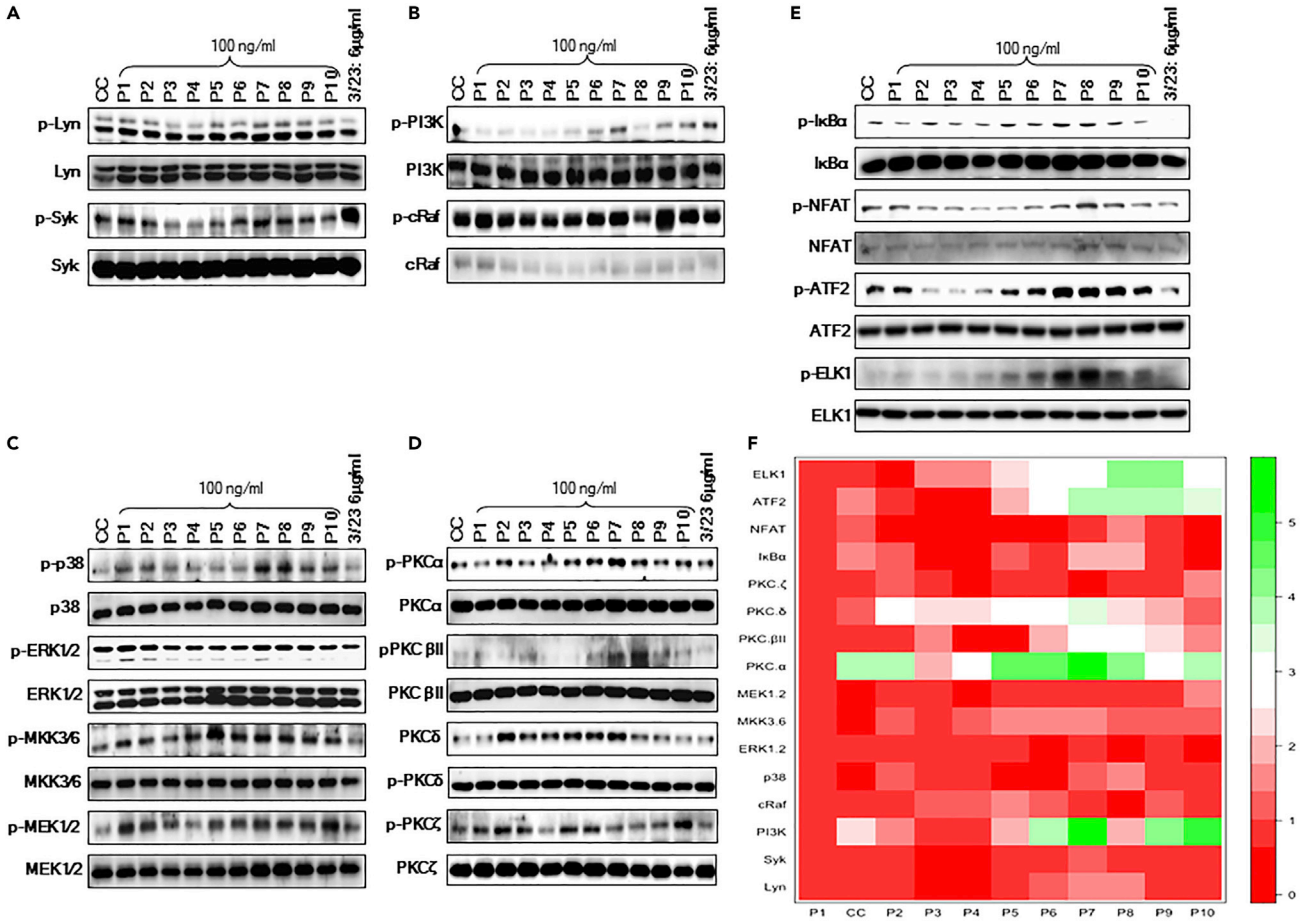

Figure 2. Stimulation with CD40L Mutant Peptides Leads to Differential Activation of CD40 Downstream Signaling Molecules and Transcription Factor in Primary Macrophages

BALB/c mice were injected (i.p.) with 3% Thioglycolate, and peritoneal macrophages were obtained on day 5 post injections. These were cultured and rested for 36 h. These were stimulated with different mutant peptides at a concentration of 100 ng/mL. αCD40 NA/LE clone 3/23 antibody (6 μg/mL) was used as an experimental control. Protein lysate was prepared and subjected to western blotting to analyze the activation of different signaling intermediates.

(A–E) (A) shows the activation of adaptor kinases Lyn and Syk, (B) shows the activation of serine/threonine kinases PI3K and c-Raf, (C) shows the activation of mitogen-activated protein kinases (MAP kinases), (D) PKCs, and (E) Transcription Factor. The immunoblots shown are representative of three independent experiments performed in duplicates showing similar results.

(F) Heatmap of different signaling molecules and the transcription factors that are activated upon stimulation with the mutant peptides. The color bar quantitatively describes the fold change for each experimental observable for CC, P2 to P10 replacement; green represents up-regulation and red represents down regulation of expression of the represented observables in a given experimental setup. The values taken to generate the heatmap are based on the mean densitometry values (shown in the Figures S2A–S2E). The experiments were performed thrice in duplicates, and results from one representative experiment are shown.

See also Figure S2.

T cell subsets and its proliferation, survival, and effector function (Habib et al., 2018), we performed macrophage-T cells co-culture. When $CD4^{+}CD44^{dim}CD25^{-}$ naive T cells from $CD40L^{-/-}$ mice were co-cultured with macrophages from C57BL/6 an increased production in IL-12 cytokine (data not shown) and decreased surface expression of PD-L1 on $CD11b^{+}$ macrophages (Figure 4A) was evident along with subsequently restored production of IFNγ and proliferation of T cells (Figures S3A and S3B) when treated with mutant peptide 7, 8, 6, and 9, respectively, in comparison with wild-type peptide as determined by FACS. Moreover, the peptides 7 and 8 were able to rescue the T cells from apoptosis as seen by Annexin-V and 7-AAD staining using FACS (Figure 4B). As CD40 was originally discovered helping B cell survival, we checked B cell survival (Koopman et al., 1997; Weller et al., 2001) of these peptide-treated sterile-sorted $CD19^{+}IgD^{+}$ naive B cells from $CD40L^{-/-}$ mice. AnnexinV/7-AAD staining showed that only Peptides 7 and 8, but not the others, enhanced survival and reduced apoptosis of B cells (Figure 4C).

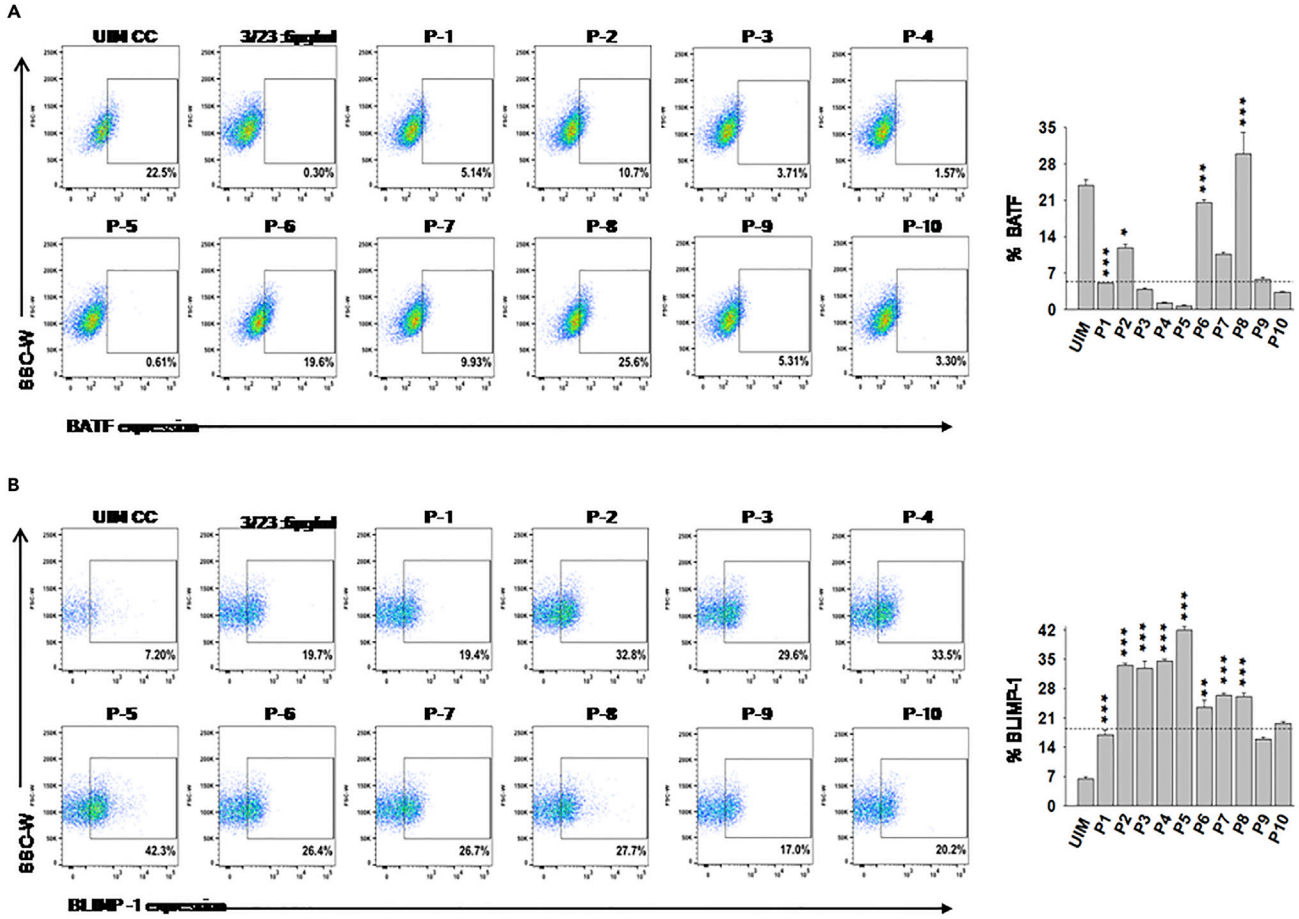

Figure 3. Activation of Transcription factors BATF and BIMP-1 is Differentially Regulated by the Mutant Peptides

Thioglycolate, 3%, was injected intraperitonial (i.p.) into BALB/c mice followed by harvesting of peritoneal macrophages after 5 days. These were cultured and rested for 36 h followed by stimulation with 100 ng/mL of mutant peptides for 48 h. The cells were harvested for FACS analysis to examine the expression of (A) BATF, a basic leucine zipper transcriptional factor ATF-like on $CD11b^+$ gated population, and the significance was drawn from three independent experiments (represented as bar graph) where the error bars show mean ± SEM, and (B) BLIMP-1, a PR domain zinc finger protein 1, on $CD11b^+$ gated population, and the significance was drawn from three independent experiments (represented in the bar graph) where the error bars show mean ± SEM. Data analysis for statistical significance was performed using one-way ANNOVA with Tukey's post-test where *$p < 0.05$, **$p < 0.01$,***$p \leq 0.001$; n.s., not significant. The results shown are representative of three independent experiments showing similar results.

Mutant Peptides Alter the Expression of CD40-Regulated Genes that Affect Cell Membrane

Because CD40 signal-induced effector functions are associated with cholesterol and ceramide in the membrane (Ghosh et al., 2002; Rub et al., 2009; Majumder et al., 2012), we checked the expression of HMG-CoA reductase (HMGCR) and ceramide synthase, the respective controlling enzymes, in BALB/c-derived elicited macrophages that were either uninfected or *L. major* infected. Peptides 6, 7, and 8 augmented HMGCR, but reduced ceramide synthase, expression, whereas peptides 2, 3, 4, 5, and 10 increased ceramide synthase, but not HMGCR, expression in both uninfected and *L. major*-infected macrophages (Figures 5A and 5B). HMGCR expression correlated with the peptides-induced alterations in the levels of cholesterol in macrophages (Figure 5C). As CD40 induces expression of inducible nitric oxide synthase (iNOS) (Awasthi et al., 2003), we checked expression of iNOS and arginase, which competes with iNOS for the common substrate L-arginine, in BALB/c-derived elicited macrophages in the presence of these peptides (Figures 5D and 5E). We observed that peptides 7 and 8, but not peptide 6, increased iNOS but reduced arginase expression, as compared with the wild-type peptide, in both uninfected and *L. major*-infected macrophages.

Because production of cytokines is associated with CD40-CD40L interaction (Mathur et al., 2004; Awasthi et al., 2003; Rub et al., 2009), we assessed the production of IL-1β, IL-6, IL-10, IL-12, TNF-α, and TGF-β by

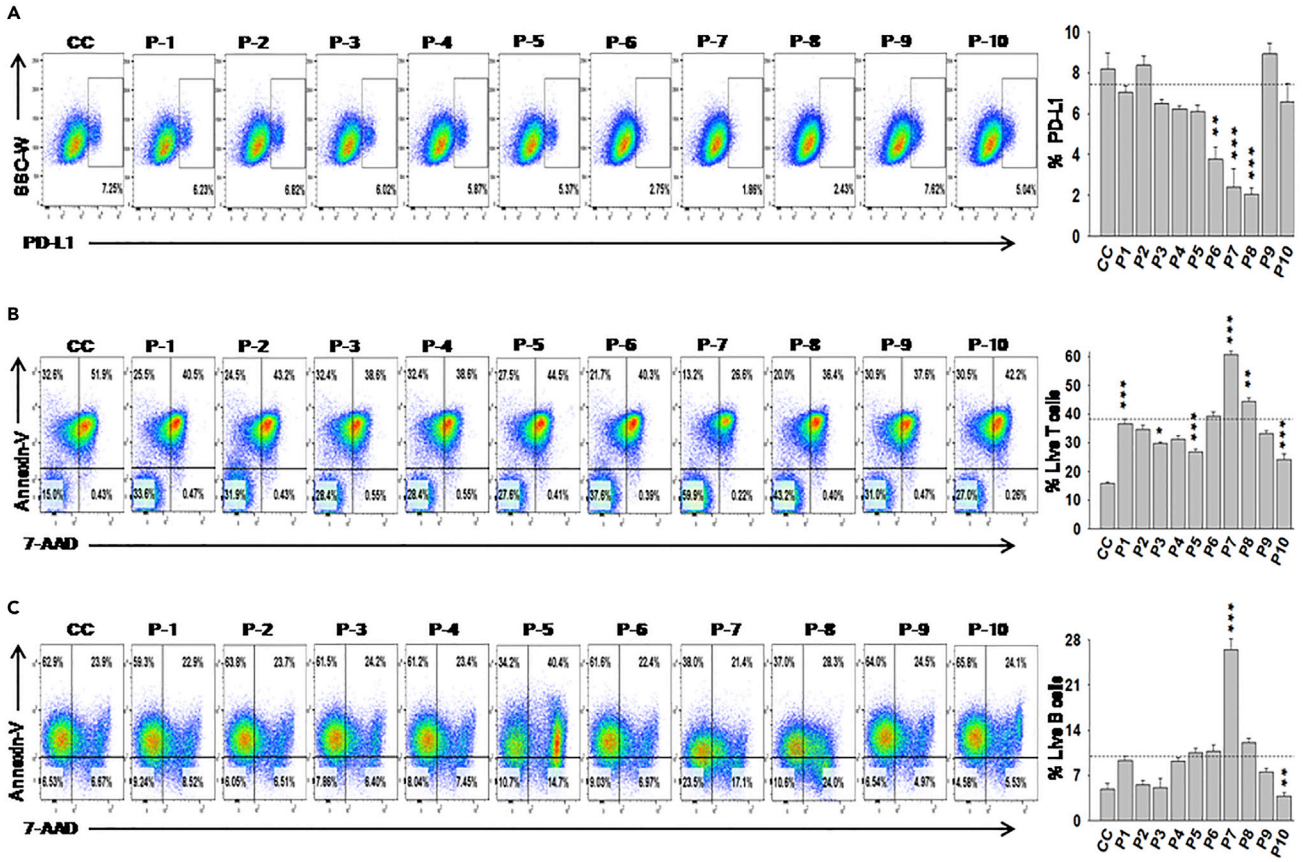

Figure 4. Peptides Can Modulate the Expression of PD-L1 and Also Aids in the Survival of T cells and B cells

C57BL/6 mice were injected (i.p.) with 3% fluid Thioglycolate media and peritoneal-derived macrophages were obtained on day 5 post injections. These macrophages were rested for 36 h and then co-cultured with sterile sorter naive $CD4^{+}CD62L^{-}CD25^{-}$T cells from $CD40L^{-/-}$ mice at a ratio of 1:3 in round bottom 96-well plates along with the respective peptides for 48 h

(A) Expression of PD-L1 on CD11b + cells of this co-culture system is shown, and the significance was drawn from three independent experiments (represented in the bar graph) where the error bars show mean ± SEM.

(B) T cell apoptosis from the co-culture system, treated with respective peptides for 48 h, using 7-AAD and AnnexinV staining gated on CD4, the significance was drawn from three independent experiments (represented in the bar graph) where the error bars show mean ± SEM. Sterile sorted $CD19^{+}IgD^{+}$ naive B cells from $CD154^{-/-}$ mice were treated with respective peptides for 48 h in round bottom 96-well plates.

(C) B cell apoptosis using 7-AAD and AnnexinV staining from the peptide-treated B cells are shown, and the significance was drawn from three independent experiments (represented in the bar graph) where the error bars show mean ± SEM. Data analysis for statistical significance was performed using one-way ANNOVA with Tukey's post-test where *p < 0.05, **p < 0.01,***p ≤ 0.001; n.s., not significant. The data shown are representative of three independent experiments.

See also Figure S3.

these CD40L peptides. Peptides 6, 7, and 8 induced higher IL-12, IL-1β, IL-6, IL-12, and TNF-α, but less IL-10 and TGF-β, production from thioglycolate-elicited peritoneal macrophages, whereas the other peptides failed to enhance these cytokines' production (Figures 6A and 6B). These results were also in line with the control of *Leishmania* amastigotes in macrophages and nitrite production (Figures 6C–6E).Thus, fine functional specificities of peptide ligands can be used for selective regulation of a receptor's functions.

Treatment with Peptide7 or Peptide8 Rescues the $CD40L^{-/-}$ Mice from *L. major* Infection

Because each interacting amino acid residue in a receptor-ligand interaction can trigger a trail of signaling events that can affect anti-leishmanial functions of CD40, we examined whether these peptides regulated anti-leishmanial functions of macrophages and in BALB/c mice. Because CD40-CD40L interaction was shown to exert anti-leishmanial functions (Mathur et al., 2004; Sudan et al., 2012; Awasthi et al., 2003; Rub et al., 2009), we assessed the anti-leishmanial functions of these peptides in CD40L-deficient mice

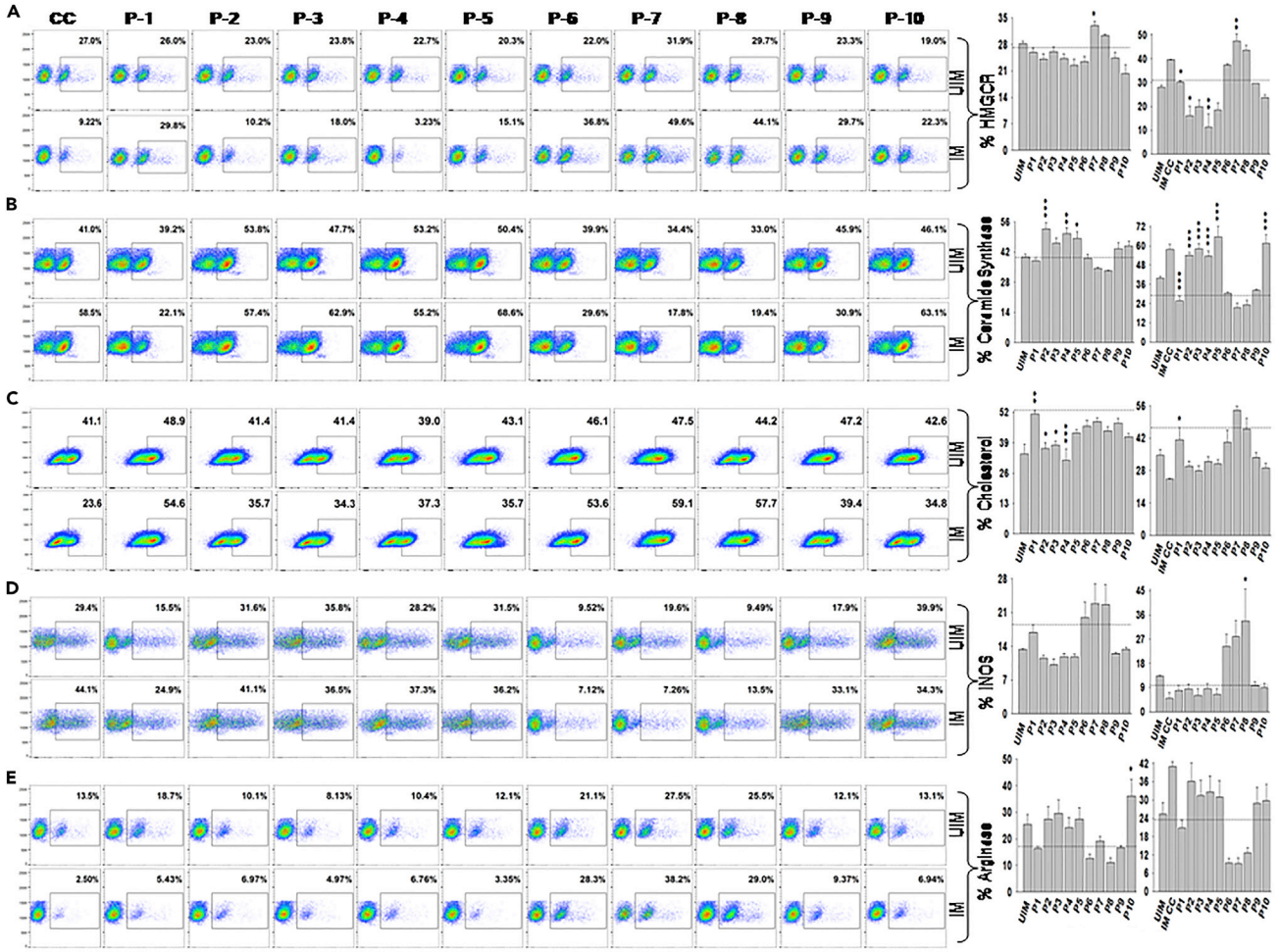

Figure 5. Functional Differences in CD40 Owing to Activation with Different Mutant Peptides of CD154

BALB/c mice were injected (i.p.) with 3% fluid Thioglycolate media, and peritoneal-derived macrophages were obtained on day 5 post injections. These were cultured and rested for 36 h. Cells were either left uninfected or infected with L. *major* promastigotes as explained in Transparent Methods. Cells were stimulated with different mutant peptides at a concentration of 100 ng/mL for 48 h. Cells were harvested and flow cytometry as explained in Transparent Methods was performed to the expression on CD11b + gated cells. Expression of (A) HMGCR controlling the rate-limiting step during Cholesterol synthesis and the significance drawn from three independent experiments (represented in the bar graph) where the error bars show mean ± SEM, (B) ceramide synthase involved in the catalysis of ceramide, and the significance was drawn from three independent experiments (represented in the bar graph) where the error bars show mean ± SEM, (C) expression of membrane cholesterol using Filipin as cholesterol-binding dye and the significance drawn from three independent experiments (represented in the bar graph) where the error bars show mean ± SEM, (D) expression of iNOS regulating the expression of NO (Nitric Oxide), and the significance was drawn from three independent experiments (represented in the bar graph) where the error bars show mean ± SEM, (E) expression of Arg-1, which is associated with the expression of NO, and the significance was drawn from three independent experiments (represented in the bar graph) where the error bars show mean ± SEM. The upper panel shows uninfected macrophages, whereas the lower panel shows infected macrophages. Data analysis for statistical significance was performed using one-way ANNOVA with Tukey's post-test where *$p < 0.05$, **$p < 0.01$, ***$p \leq 0.001$; n.s., not significant. Results shown are representative of three independent experiments.

on C57BL/6 background. We infected these mice with *L. major* promastigotes at the hind footpad, followed by treatment with the peptides on days 1, 3, 5, and 7 post infection. Maximum protection against the infection was offered by peptides 7 and 8, followed by peptides 6 and 9 (Figures 7A and S4A). The real-time PCR with the RNA extracted from the draining lymph node cells showed distinct profiles of IL-10, IL-12, IL-4, IFN-γ, IL-1β, IL-6, TNF-α, Arginase, and NO (Figures 7B and S4B). When pulsed with leishmanial antigens, lymph node cells from the peptide 7- or 8-treated mice showed reduced IL-10 production but heightened IL-12 and IFN-γ (Figure 7C). The lymph node cells from the peptides 7 and 8-treated mice efficiently cleared parasites from the co-cultured *L. major*-infected macrophages (Figure S4C); peptides 6 and 9 had less efficiency but the other peptides did not have any effect. This was further supported by the increased

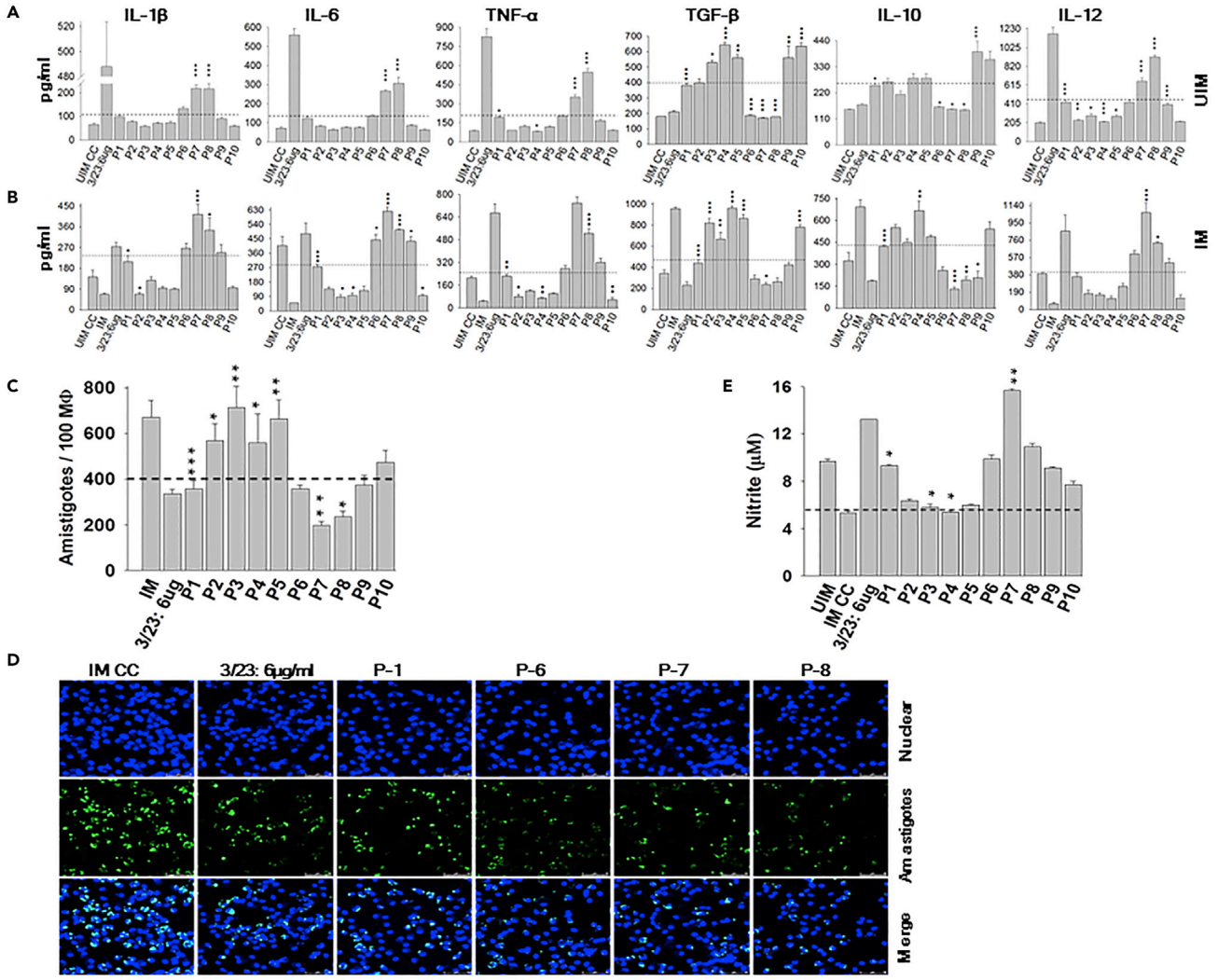

Figure 6. Mutant Peptides of CD154 Can Induce Differential Expression of Cytokine in Both Un-infected and Infected Macrophages Which Also Helps in the Control of Intracellular Parasites

BALB/c mice were injected (i.p.) with 3% fluid Thioglycolate media and peritoneal-derived macrophages were obtained on day 5 post injections. These were cultured and rested for 36 h. Cells were either left uninfected or infected with L. *major* promastigotes for 36 h as explained in Transparent Methods. Cells were stimulated with different mutant peptides at a concentration of 100 ng/mL for 72 h and the supernatant was assessed for cytokine production using ELISA.

(A) Shows the expression of IL-1β, IL-6, TNF-α, TGF-β, IL-10, and IL-12 in uninfected mice macrophages.

(B) Shows the expression of these cytokines in *L. major*-infected mice macrophages. The data shown are representative of three independent experiments and error bars show mean ± SEM. Data analysis for statistical significance was performed using one-way ANNOVA with Tukey's post-test where *$p < 0.05$, **$p < 0.01$, ***$p \leq 0.001$; n.s., not significant. BALB/c mice were injected (i.p.) with 3% fluid Thioglycolate media and peritoneal-derived macrophages were obtained on day 5 post injections. These were cultured and rested for 36 h. Cells were either left uninfected or infected with L. *major* promastigotes for 36 h as explained in Transparent Methods. Cells were stimulated with different mutant peptides at a concentration of 100 ng/mL for 72 h

(C) Shows the numbers of *L. major* amistigotes/100 macrophages (parasite load assay explained in materials and methods) in infected macrophages using Giemsa staining. The data shown are representative of three independent experiments and error bars show mean ± SEM. Data analysis for statistical significance was performed using one-way ANNOVA with Tukey's post-test where *$p < 0.05$, **$p < 0.01$,***$p \leq 0.001$; n.s., not significant.

(D) Resting macrophages were infected with CFSE-labeled stationary phase *L. major* promastigotes for 8 h. Unbound parasites were washed and cells were kept for 48 h. Respective peptides (P1, P6, P7, and P8) 100 ng/mL and αCD40 NA/LE clone 3/23 antibody 6 μg/mL were used to stimulate the cells for 72 h after which cells were stained for the nuclear stain using Hoechst 33342 and confocal images were captured on Leica SPII machine under 100X oil immersion lens. The experiments were performed at least thrice, and one of the representatives is shown in the figure.

(E) NO production in the culture supernatant of *L. major*-infected macrophages stimulated with the peptide for 72 h (100 ng/mL) was assessed using Griess reagent. The data shown are representative of three independent experiments and error bars show mean ± SEM.

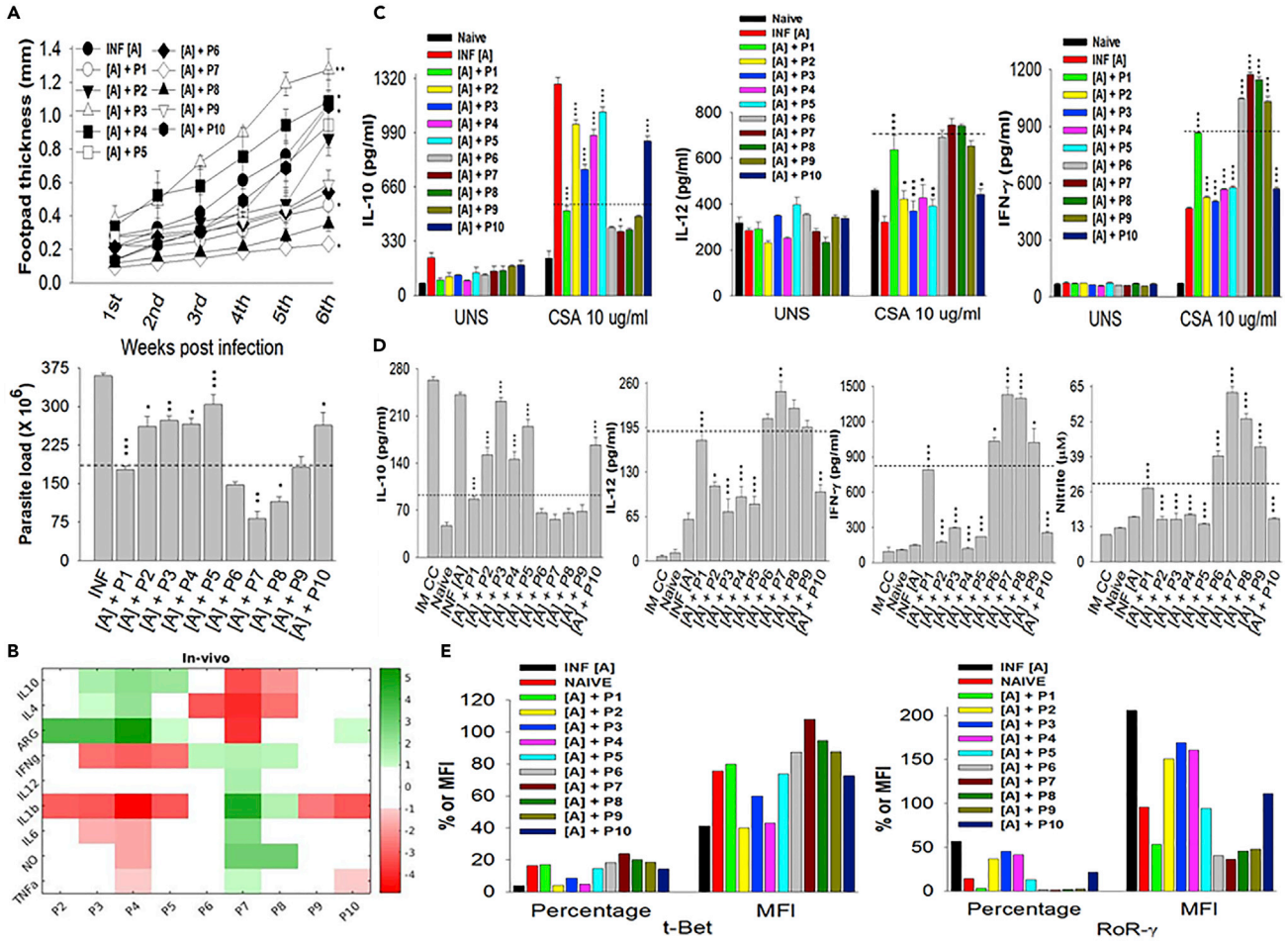

Figure 7. Treatment with Peptides 7 and 8 Confers Protection against *L. major* in CD40L-Deficient Mice

Stationary phase *L. major* promastigotes (2×10^6) were injected subcutaneous injection (s.c.) at the hind footpad of $CD40L^{-/-}$ mice on a C57BL/6 background. Mutant peptide at a dose of 6 mg/kg/mice in HBSS was administered to the mice (i.p.) mode on day 1, 3, 5, and 7 post infection.

(A) The footpad swelling of the infected mice (n = 5) was monitored till sixth week and shown as line graph (upper panel). Mice were sacrificed on the sixth week and the popliteal lymph node was collected and the parasite burden was checked (lower panel). Results shown are representative of three independent experiments with similar results.

(B)Heatmap showing relative expression of different pro- and anti-inflammatory cytokines elements from the lymphocytes obtained from the mice treated with CD154 mutants with P2 to P10 replacement. Fold change over P1 (as explained in Methods) is shown here on a log2 scale. The color bar quantitatively describes the fold change for each experimental observable for P2 to P10 replacement; green represents up-regulation and red represents down-regulation of expression of the represented observables in a given experimental setup. The results shown are representative of three independent experiments showing similar results. Lymphocytes were cultured in the presence of Crude Soluble Antigen (CSA) for 72 h and the supernatant was used to check the expression of cytokines IL10, IL12, and IFN-γ.

(C) The data shown are representative of three independent experiments and error bars show mean ± SEM. Statistical significance of the differences between the means was assessed by one-way ANNOVA with Tukey's post-test where *p < 0.05, **p < 0.01, ***p ≤ 0.001; n.s., not significant. C57BL/6 macrophages were infected with stationary phase *L. major* promastigotes at a macrophage:parasite ratio of 1:10 for 8 h. Unbound parasites were washed and macrophages were rested for 48 h. Lymphocytes obtained from the peptide-treated mice were co-cultured with these *L. major*-infected macrophages along with CSA (10 μg/mL) for 72 h, and the supernatant was subjected to cytokine ELISA.

(D) IL10, IL12, IFN-γ, and NO contents in the supernatants are shown. The data shown are representative for three independent experiments and error bars show mean ± SEM. Data analysis for statistical significance was performed using one-way ANNOVA with Tukey's post-test where *p < 0.05, **p < 0.01,***p ≤ 0.001; n.s., not significant.

(E) The lymphocytes from similar treated group were pooled and subjected to FACS analysis to examine the expression of t-Bet expressing Th1 and RoR-γt expressing Th17 gated on $CD4^+CD44^+CD62L^-$ T cell subsets. The percentage positive cells and the mean fluorescent intensity (MFI) in the gated population are shown. The data shown are representative of three independent experiments showing similar results.

See also Figure S4.

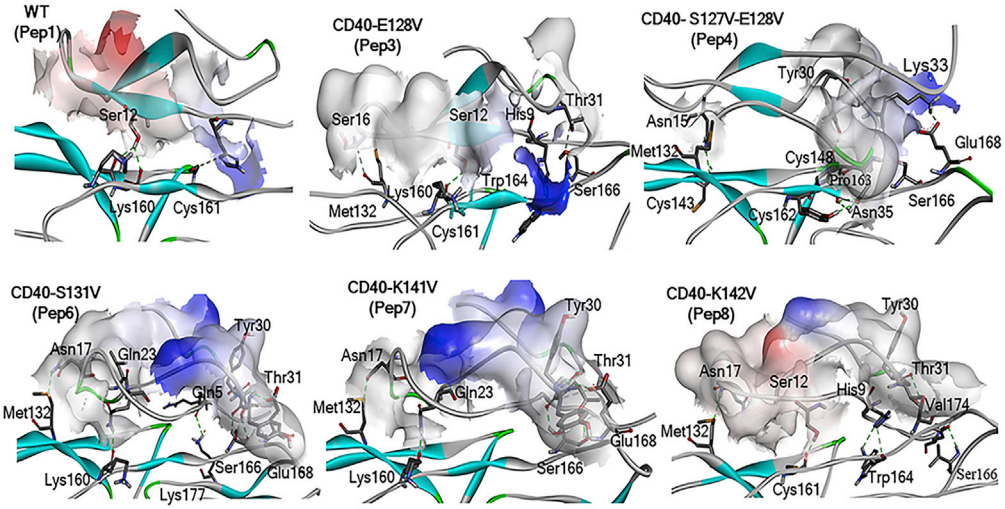

Figure 8. CD40-CD40L (41-mer Peptides) Predicted Docking Model

The electron cloud model of the structural features of the CD40 receptor and CD40L 41-mer peptides docked complexes. The color-coded structures are according to secondary structural features, and the cloud color depicts surface charge potential (red, negative charge; blue, positive charge). Interactions are shown as green dash line for classical hydrogen bonds, orange dash line for salt bridges. Comparative docking shows different interacting partners among complexes and against wild-type peptide-CD40 complex. Among specific interacting patterns in each complex, CD40-Pep6, CD40-Pep7, and CD40-Pep8 share Asn17-Met132, Ty30-Ser166, and Thr31-Glu168 interactions. Each interacting region shows distinctive impact on the complex surface charge potential. See also Figures S5 and S6.

production of pro-inflammatory cytokine IL-12, IFN-γ, and nitrite production along with reduced IL-10 production (Figure 7D). These lymph node cells from the mice treated with peptide 7 or peptide 8 had higher t-Bet^{+}CD4^{+} T cells but fewer RoRγt^{+}CD4^{+} T cells (Figures 7E and S4D). These results show that the messages encoded in a given residue can be altered by residue-specific mutations to generate a host-protective agonist of CD40L displaying unique collective cytokine expression profiles.

Mutations Affect Electrostatic Surface Potential and Predict Variable Interfacing Contacts

Because conformational complementarity is at the root of all receptor-ligand interactions, we first tested whether the peptides had any structural disorders. Analyses of the structures by DisEMBL (Linding et al., 2003a), GlobPlot (Linding et al., 2003b), and PONDR (Xue et al., 2010) did not detect any structural disorder. Next, analyses of the secondary structures of these peptides by Molprobity (Williams et al., 2018) and PROBE and visualization by KiNG (Chen et al., 2009) identified that these substitutions brought subtle characteristic changes in their structures (Figure S5). Electrostatic surface potential charge analysis identified induction of positive electrostatic surface potential in Pep2, Pep3, and Pep6 but negative surface potential in the Pep7 and Pep10, as compared with wild-type peptide (Figure S6). Hydrogen bond types (N-H … O, O-H … O, and C-H … O) were found between the residues of receptor and ligand. The S127 (Ser12) residue of peptides is prominent in all the interactions. Among all peptides, a common interaction pattern existed between Y30-E168 and T31-S166 of the CD40-Pep6, CD40-Pep7, and CD40-Pep8 receptor-ligand dockings and peptide (Figure 8).

DISCUSSION

The classical studies on the interactions between peptide hormones and their transmembrane receptors involved mutation of a length of the gene or site-directed mutagenesis to ascertain that a particular stretch of the primary structure or specific amino acid of the hormone was required for the chosen assay to determine the peptide hormone activity. Such approaches suffered from the assumption that the chosen assay for the hormone activity represented all activities of the hormone, although the hormones used to be known as pleiotropic. Therefore, whether each of the function-inducing amino acids on the hormone would encode a specific message and would thus collectively impart the pleiotropic functions onto the hormone remained unknown. Thus, although transmembrane receptor-ligand interactions involve interactions

between specific amino acids in ligand and the receptor, their specific roles distributed in different functions triggered by the receptor is never described. Indeed, the mutation of any of the reported nine residues led to XIgM syndrome suggesting their functional redundancy. The alternative possibility is that each of these nine amino acid residues triggers different signaling pathways that converge onto the mainstay of the receptor signaling such that the messages could be different but the final effector functions would be same. In this case, therefore, each amino acid substitution to 115–155 peptide ligand should have resulted in similar changes in the signaling and functions. By contrast, we decipher distinct collective profiles of changes for each of the amino acids substituted in the mutant CD40L. Our data suggest that each of these residues triggers specific CD40 signaling and induces a specific combination of cytokines and other effector responses in addition to the B cell survival. These residue-specific changes in the function were also observed in *Leishmania*-infected macrophage, which targets the CD40-associated signaling and gene expression. The study by Dadgostar et al. suggested differential regulation of CD40-associated genes as a virtue of independent, synergistic, and redundant control by CD40 stimulation (Dadgostar et al., 2002); however, the factors that dictate the aforementioned were not examined. We propose these factors to be individual residues having an independent, collective, and redundant control over the signaling, the output of which is a specific set of function, as evident by differential signaling and effector functions.

Although any of these mutations resulted in impaired IgM class switching to IgG in B cells (Bajorath et al., 1996; Thusberg and Vihinen, 2007), here a mutation does not necessarily impair all functions similarly in macrophages. Whether these peptides will show similar alterations in B cells proliferation, cytokine production, and phenotypic changes requires an independent study, but herein the B cell survival was not equally affected by all mutant CD40-L peptides: peptide 7 and peptide 8 did rescue the B cells from apoptosis. As B cells and macrophages belong to different lineages of hematopoietic cells—lymphocytic and myeloid, respectively—the reason for differences between B cells and macrophages could simply be differences in constitutive expression of genes or cell-specific genetic repression program. The other possible mechanisms of the observed difference could be many: differences in the membrane lipids in which the receptor is embedded, expression of the receptor-associated molecules or the expression of signaling molecules, or the threshold of activation of these molecules, particularly those involved in cell survival or even in the post-translational modification of proteins or cell-specific protein expressions. However, an independent study is required to settle how CD40 functions in B cells can be different from that in macrophages.

Structurally, such mutations may represent altered positioning of each of the other contact residues with their counterparts in CD40 receptor or localized disruption of the residue-specific interactions between the target (substituted) residue on the ligand and its interacting residue on CD40. As we did not observe any major structural changes in any of the substituted peptides, it is unlikely that one substitution alters all interactions. As a result, it is very likely that the substituted amino acid will alter only its specific interaction and will therefore alter the functions associated with this residue. Compared with the functions associated with the wild-type CD40L, each mutation caused specific functional alteration profiles that collectively assigned the functional specificity to the residue. Moreover, the residue-specific interaction of CD40L with other receptors such as integrin family and sharing common signaling intermediates like TRAFs and MAPKs would modulate the signaling pathway and signal strength (El Fakhry et al., 2012; Léveillé et al., 2007).Therefore, the message encoded in each of the residues in CD40L peptides relates to the collective profiles of functions, which could be the result of specific combinations of signaling.

It is plausible that CD40L peptides' binding to CD40 induces a wave of structural changes in CD40 and is relayed to the intracellular domain where the signaling molecules including adaptors such as TRAF are recruited (McWhirter et al., 1999; Ahonen et al., 2002). Contingent upon this signalosome complex, the subsequent signaling network is determined. CD40 is reported to bind TRAFs with varying avidity through the TRAF-binding domains, which are exposed owing to ligand binding activation and CD40 clustering (Pullen et al., 1998, 1999a, 1999b). The stoichiometry of the TRAF-binding domains depends on the interacting residues of CD40L-CD40 interphase resulting in the complete or restricted exposure of this domain thereby differentially recruiting TRAF protein having different signaling outcomes. The presence of preformed CD40 clusters with itself and another tumor necrosis factor receptor (TNFR) family can also change the binding stoichiometry with incoming residues on the ligand. It is plausible that the message encoded in one residue of the ligand is to induce very specific profiles of structural changes to the receptor eventuating

in combinations of different functions with specific amplitude and kinetic profiles. However, such cryptographic references are yet to appear. To the best of our knowledge, this is the first report that implies physical form of cryptography in a biological system.

These peptides also differentially regulate the induction of PD-L1, an inhibitory molecule that can be blocked to derive an anti-leishmanial function (Habib et al., 2018; Bhadra et al., 2011), and the peptides that down-regulate PD-L1 also elicit host-protective anti-leishmanial T cell response. A specific residue in a ligand can thus have functional integration of the elicited signals with the subsequent events that can be immuno-regulatory. Therefore, our data imply that, instead of blocking the downstream PD-L1-mediated pro-leishmanial functions, the therapy can be the upstream choice of engineered ligands with the residues that reduce PD-L1 expression. The identification of different pockets on the CD40 receptor can be exploited for targeted signaling modulations that are elicited by CD40 opening up a new avenue for the structure-function relationship for targeted drug discovery (Vaitaitis et al., 2014). The use of small peptides and molecules will also overcome the limitations such as thromboembolic unfavorable effects associated with use of anti-CD40 antibody (Xie et al., 2014). Our data not only uncover the novel message encoding in each amino acid and its decoding by intracellular signaling but also, as they lead to residue-specific effector functions profile, provide a scientific rationale for designing an immuno-therapeutic strategy. In essence, this is the first demonstration of the residue-specific message encoding system and decoding of messages by signaling intermediates. At this moment, the technical limitations do not allow mapping the atomic changes in the interacting residues. An online mapping of such changes in the interacting receptor and its ligand will lead to the next level of cryptography.

Limitations of the Study

In this study we have shown that residues trigger specific CD40 signaling and induce a specific combination of cytokines and other effector responses in addition to the B cell survival. Although any of these mutations resulted in impaired IgM class switching to IgG in B cells, here a mutation does not necessarily impair all functions similarly in macrophages. However, we do not know whether these peptides will show analogous alterations in B cells proliferation, cytokine production, and phenotypic changes for which an independent study will be required. The reason for differences between B cells and macrophages could be many: differences in the membrane lipids in which the receptor is embedded, expression of the receptor-associated molecules or the expression of signaling molecules, or the threshold of activation of these molecules, particularly those involved in cell survival or even in the post-translational modification of proteins or cell-specific protein expressions. In addition, the involvement of these residues during germinal center formation will be fateful in the affinity maturation and memory T cell formation owing to differential signaling and activation of genes resulting in recruitment of follicular dendritic cells, a prerequisite for germinal center formation. However, an independent study is necessary to reconcile how CD40 functions in B cells can be dissimilar from that in macrophages.

Resource Availability

Lead Contact

Further information is availabe from the Lead Contact, Bhaskar Saha (bhaskar211964@yahoo.com).

Materials Availability

The study did not generate new unique reagents which can be made avaiabe, therefore its not required.

Data and Code Availability

The study did not use any unpublished custom code, software, or algorithm that is central to supporting the main claims of the paper, therefore its not required.

METHODS

All methods can be found in the accompanying Transparent Methods supplemental file.

SUPPLEMENTAL INFORMATION

Supplemental Information can be found online at https://doi.org/10.1016/j.isci.2020.101441.

ACKNOWLEDGMENTS

The work has been financially assisted by a grant from DST-UKIERI (DST/INT/UK/2016/P-123) and the JC Bose National Fellowship by the Department of Science and Technology, Government of India to B.S.

AUTHOR CONTRIBUTIONS

A.Y.S., S.Z., M.K.J., and H.M. performed the experiments. S.K.G. performed all Bioinformatics analyses. U.S. performed the mathematical modeling and generated the heatmaps. B.S. and A.Y.S. designed the experiments and composed the manuscript.

DECLARATION OF INTERESTS

Authors do not have any conflict of interest.

Received: February 18, 2020
Revised: July 15, 2020
Accepted: August 3, 2020
Published: September 25, 2020

REFERENCES

Ahonen, C.L., Manning, E.M., Erickson, L.D., O'connor, B.P., Lind, E.F., Pullen, S.S., Kehry, M.R., and Noelle, R.J. (2002). The CD40-TRAF6 axis controls affinity maturation and the generation of long-lived plasma cells. Nat. Immunol. *3*, 451–456.

An, H.-J., Kim, Y.J., Song, D.H., Park, B.S., Kim, H.M., Lee, J.D., Paik, S.-G., Lee, J.-O., and Lee, H. (2011). Crystallographic and mutational analysis of the CD40-CD154 complex and its implications for receptor activation. J. Biol. Chem. *286*, 11226–11235.

Awasthi, A., Mathur, R., Khan, A., Joshi, B.N., Jain, N., Sawant, S., Boppana, R., Mitra, D., and Saha, B. (2003). CD40 signaling is impaired in L. major-infected macrophages and is rescued by a p38MAPK activator establishing a host-protective memory T cell response. J. Exp. Med. *197*, 1037–1043.

Baccam, M., Woo, S.Y., Vinson, C., and Bishop, G.A. (2003). CD40-mediated transcriptional regulation of the IL-6 gene in B lymphocytes: involvement of NF-kappa B, AP-1, and C/EBP. J. Immunol. *170*, 3099–3108.

Bajorath, J. (1998). Detailed comparison of two molecular models of the human CD40 ligand with an X-ray structure and critical assessment of model-based mutagenesis and residue mapping studies. J. Biol. Chem. *273*, 24603–24609.

Bajorath, J., Chalupny, N.J., Marken, J.S., Siadak, A.W., Skonier, J., Gordon, M., Hollenbaugh, D., Noelle, R.J., Ochs, H.D., and Aruffo, A. (1995). Identification of residues on CD40 and its ligand which are critical for the receptor-ligand interaction. Biochemistry *34*, 1833–1844.

Bajorath, J., Seyama, K., Nonoyama, S., Ochs, H.D., and Aruffo, A. (1996). Classification of mutations in the human CD40 ligand, gp39, that are associated with X-linked hyper IgM syndrome. Protein Sci. *5*, 531–534.

Bhadra, R., Gigley, J.P., and Khan, I.A. (2011). Cutting edge: CD40-CD40 ligand pathway plays a critical CD8-intrinsic and -extrinsic role during rescue of exhausted CD8 T cells. J. Immunol. *187*, 4421–4425.

Busch, R., Murti, K., Liu, J., Patra, A.K., Muhammad, K., Knobeloch, K.P., Lichtinger, M., Bonifer, C., Wortge, S., Waisman, A., et al. (2016). NFATc1 releases BCL6-dependent repression of CCR2 agonist expression in peritoneal macrophages from *Saccharomyces cerevisiae* infected mice. Eur. J. Immunol. *46*, 634–646.

Chen, V.B., Davis, I.W., and Richardson, D.C. (2009). KING (Kinemage, Next Generation): a versatile interactive molecular and scientific visualization program. Protein Sci. *18*, 2403–2409.

Dadgostar, H., Zarnegar, B., Hoffmann, A., Qin, X.-F., Truong, U., Rao, G., Baltimore, D., and Cheng, G. (2002). Cooperation of multiple signaling pathways in CD40-regulated gene expression in B lymphocytes. Proc. Natl. Acad. Sci. U S A *99*, 1497–1502.

Di Roberto, R.B., Chang, B., and Peisajovich, S.G. (2017). The directed evolution of ligand specificity in a GPCR and the unequal contributions of efficacy and affinity. Sci. Rep. *7*, 16012.

El Fakhry, Y., Alturaihi, H., Yacoub, D., Liu, L., Guo, W., Leveillé, C., Jung, D., Khzam, L.B., Merhi, Y., Wilkins, J.A., et al. (2012). Functional interaction of CD154 protein with α5β1 integrin is totally independent from its binding to αIIbβ3 integrin and CD40 molecules. J. Biol. Chem. *287*, 18055–18066.

Elgueta, R., Benson, M.J., de Vries, V.C., Wasiuk, A., Guo, Y., and Noelle, R.J. (2009). Molecular mechanism and function of CD40/CD40L engagement in the immune system. Immunol. Rev. *229*, 152–172.

Elgueta, R., De Vries, V.C., and Noelle, R.J. (2010). Chapter 51 - mechanisms of CD40 signaling in the immune system. In Handbook of Cell Signaling, Second Edition, R.A. Bradshaw and E.A. Dennis, eds. (Academic Press), pp. 353–358.

Garber, E., Su, L., Ehrenfels, B., Karpusas, M., and Hsu, Y.-M. (1999). CD154 variants associated with hyper-IgM syndrome can form oligomers and trigger CD40-mediated signals. J. Biol. Chem. *274*, 33545–33550.

Ghosh, S., Bhattacharyya, S., Sirkar, M., Sa, G.S., Das, T., Majumdar, D., Roy, S., and Majumdar, S. (2002). *Leishmania donovani* suppresses activated protein 1 and NF-kappaB activation in host macrophages via ceramide generation: involvement of extracellular signal-regulated kinase. Infect. Immun. *70*, 6828–6838.

Habib, S., El Andaloussi, A., Elmasry, K., Handoussa, A., Azab, M., Elsawey, A., Al-Hendy, A., and Ismail, N. (2018). PDL-1 blockade prevents T cell exhaustion, inhibits autophagy, and promotes clearance of *Leishmania donovani*. Infect. Immun. *86*, e00019-18.

Karpusas, M., Lucci, J., Ferrant, J., Benjamin, C., Taylor, F.R., Strauch, K., Garber, E., and Hsu, Y.-M. (2001). Structure of CD40 ligand in complex with the fab fragment of a neutralizing humanized antibody. Structure *9*, 321–329.

Khan, S., Alonso, L., Roduit, C., Bandyopadhyay, S., Singh, S., Saha, S., Tacchini-Cottier, F., Roy, S., Dietler, G., Kasas, S., et al. (2012). Differential peptide binding to CD40 evokes counteractive responses. Hum. Immunol. *73*, 465–469.

Khan, T.H., Srivastava, N., Srivastava, A., Sareen, A., Mathur, R.K., Chande, A.G., Musti, K.V., Roy, S., Mukhopadhyaya, R., and Saha, B. (2014). SHP-1 plays a crucial role in CD40 signaling reciprocity. J. Immunol. *193*, 3644–3653.

Koopman, G., Keehnen, R.M.J., Lindhout, E., Zhou, D.F.H., De Groot, C., and Pals, S.T. (1997). Germinal center B cells rescued from apoptosis by CD40 ligation or attachment to follicular dendritic cells, but not by engagement of surface immunoglobulin or adhesion receptors, become resistant to CD95-induced apoptosis. Eur. J. Immunol. *27*, 1–7.

Kumanogoh, A., Wang, X., Lee, I., Watanabe, C., Kamanaka, M., Shi, W., Yoshida, K., Sato, T., Habu, S., Itoh, M., et al. (2001). Increased T cell autoreactivity in the absence of CD40-CD40 ligand interactions: a role of CD40 in regulatory T cell development. J. Immunol. *166*, 353–360.

Laporte, S.L., Juo, Z.S., Vaclavikova, J., Colf, L.A., Qi, X., Heller, N.M., Keegan, A.D., and Garcia, K.C. (2008). Molecular and structural basis of cytokine receptor pleiotropy in the interleukin-4/13 system. Cell *132*, 259–272.

Léveillé, C., Bouillon, M., Guo, W., Bolduc, J., Sharif-Askari, E., El-Fakhry, Y., Reyes-Moreno, C., Lapointe, R., Merhi, Y., Wilkins, J.A., and Mourad, W. (2007). CD40 ligand binds to α5β1 integrin and triggers cell signaling. J. Biol. Chem. *282*, 5143–5151.

Liao, J., Humphrey, S.E., Poston, S., and Taparowsky, E.J. (2011). Batf promotes growth arrest and terminal differentiation of mouse myeloid leukemia cells. Mol. Cancer Res. *9*, 350–363.

Linding, R., Jensen, L.J., Diella, F., Bork, P., Gibson, T.J., and Russell, R.B. (2003a). Protein disorder prediction: implications for structural proteomics. Structure *11*, 1453–1459.

Linding, R., Russell, R.B., Neduva, V., and Gibson, T.J. (2003b). GlobPlot: exploring protein sequences for globularity and disorder. Nucleic Acids Res. *31*, 3701–3708.

Macchi, P., Villa, A., Strina, D., Sacco, M.G., Morali, F., Brugnoni, D., Giliani, S., Mantuano, E., Fasth, A., and Andersson, B. (1995). Characterization of nine novel mutations in the CD40 ligand gene in patients with X-linked hyper IgM syndrome of various ancestry. Am. J. Hum. Genet. *56*, 898–906.

Majumder, S., Dey, R., Bhattacharjee, S., Rub, A., Gupta, G., Bhattacharyya Majumdar, S., Saha, B., and Majumdar, S. (2012). Leishmania-induced biphasic ceramide generation in macrophages is crucial for uptake and survival of the parasite. J. Infect. Dis. *205*, 1607–1616.

Martin, S., Agarwal, R., Murugaiyan, G., and Saha, B. (2010). CD40 expression levels modulate regulatory T cells in *Leishmania donovani* infection. J. Immunol. *185*, 551–559.

Mathur, R.K., Awasthi, A., Wadhone, P., Ramanamurthy, B., and Saha, B. (2004). Reciprocal CD40 signals through p38MAPK and ERK-1/2 induce counteracting immune responses. Nat. Med. *10*, 540–544.

McWhirter, S.M., Pullen, S.S., Holton, J.M., Crute, J.J., Kehry, M.R., and Alber, T. (1999). Crystallographic analysis of CD40 recognition and signaling by human TRAF2. Proc. Natl. Acad. Sci. U S A *96*, 8408–8413.

Murugaiyan, G., Agrawal, R., Mishra, G.C., Mitra, D., and Saha, B. (2006). Functional dichotomy in CD40 reciprocally regulates effector T cell functions. J. Immunol. *177*, 6642–6649.

Murugaiyan, G., Agrawal, R., Mishra, G.C., Mitra, D., and Saha, B. (2007). Differential CD40/CD40L expression results in counteracting antitumor immune responses. J. Immunol. *178*, 2047–2055.

Pullen, S.S., Dang, T.T.A., Crute, J.J., and Kehry, M.R. (1999a). CD40 Signaling through Tumor Necrosis Factor Receptor-associated Factors (TRAFs): binding site specificity and activation of downstream pathways by distinct TRAFs. J. Biol. Chem. *274*, 14246–14254.

Pullen, S.S., Labadia, M.E., Ingraham, R.H., Mcwhirter, S.M., Everdeen, D.S., Alber, T., Crute, J.J., and Kehry, M.R. (1999b). High-affinity interactions of tumor necrosis factor receptor-associated factors (TRAFs) and CD40 require TRAF trimerization and CD40 multimerization. Biochemistry *38*, 10168–10177.

Pullen, S.S., Miller, H.G., Everdeen, D.S., Dang, T.T.A., Crute, J.J., and Kehry, M.R. (1998). CD40—Tumor necrosis factor receptor-associated factor (TRAF) Interactions: regulation of CD40 signaling through multiple TRAF binding sites and TRAF hetero-oligomerization. Biochemistry *37*, 11836–11845.

Reichmann, G., Walker, W., Villegas, E.N., Craig, L., Cai, G., Alexander, J., and Hunter, C.A. (2000). The CD40/CD40 ligand interaction is required for resistance to toxoplasmic encephalitis. Infect. Immun. *68*, 1312–1318.

Root-Bernstein, R.S. (2005). Peptide self-aggregation and peptide complementarity as bases for the evolution of peptide receptors: a review. J. Mol. Recognit. *18*, 40–49.

Roy, A., Kucukural, A., and Zhang, Y. (2010). I-TASSER: a unified platform for automated protein structure and function prediction. Nat. Protoc. *5*, 725–738.

Roy, S., Guler, R., Parihar, S.P., Schmeier, S., Kaczkowski, B., Nishimura, H., Shin, J.W., Negishi, Y., Ozturk, M., Hurdayal, R., et al. (2015). Batf2/Irf1 induces inflammatory responses in classically activated macrophages, lipopolysaccharides, and mycobacterial infection. J. Immunol. *194*, 6035–6044.

Rub, A., Dey, R., Jadhav, M., Kamat, R., Chakkaramakkil, S., Majumdar, S., Mukhopadhyaya, R., and Saha, B. (2009). Cholesterol depletion associated with *Leishmania major* infection alters macrophage CD40 signalosome composition and effector function. Nat. Immunol. *10*, 273–280.

Schröfelbauer, B., and Hoffmann, A. (2011). How do pleiotropic kinase hubs mediate specific signaling by TNFR superfamily members? Immunol. Rev. *244*, 29–43.

Severa, M., Islam, S.A., Waggoner, S.N., Jiang, Z., Kim, N.D., Ryan, G., Kurt-Jones, E., Charo, I., Caffrey, D.R., Boyartchuk, V.L., et al. (2014). The transcriptional repressor BLIMP1 curbs host defenses by suppressing expression of the chemokine CCL8. J. Immunol. *192*, 2291–2304.

Seyama, K., Nonoyama, S., Gangsaas, I., Hollenbaugh, D., Pabst, H.F., Aruffo, A., and Ochs, H.D. (1998). Mutations of the CD40 ligand gene and its effect on CD40 ligand expression in patients with X-linked hyper IgM syndrome. Blood *92*, 2421–2434.

Siddiq, M.A., Hochberg, G.K., and Thornton, J.W. (2017). Evolution of protein specificity: insights from ancestral protein reconstruction. Curr. Opin. Struct. Biol. *47*, 113–122.

Spangler, J.B., Moraga, I., Mendoza, J.L., and Garcia, K.C. (2015). Insights into cytokine-receptor interactions from cytokine engineering. Annu. Rev. Immunol. *33*, 139–167.

Starr, T.N., and Thornton, J.W. (2016). Epistasis in protein evolution. Protein Sci. *25*, 1204–1218.

Sudan, R., Srivastava, N., Pandey, S.P., Majumdar, S., and Saha, B. (2012). Reciprocal regulation of protein kinase C isoforms results in differential cellular responsiveness. J. Immunol. *188*, 2328–2337.

Suttles, J., Milhorn, D.M., Miller, R.W., Poe, J.C., Wahl, L.M., and Stout, R.D. (1999). CD40 signaling of monocyte inflammatory cytokine synthesis through an ERK1/2-dependent pathway: a target of interleukin (IL)-4 and IL-10 anti-inflammatory action. J. Biol. Chem. *274*, 5835–5842.

Thornton, J.W. (2001). Evolution of vertebrate steroid receptors from an ancestral estrogen receptor by ligand exploitation and serial genome expansions. Proc. Natl. Acad. Sci. U S A *98*, 5671–5676.

Thusberg, J., and Vihinen, M. (2007). The structural basis of hyper IgM deficiency – CD40L mutations. Protein Eng. Des. Sel. *20*, 133–141.

Uchida, J., Yasui, T., Takaoka-Shichijo, Y., Muraoka, M., Kulwichit, W., Raab-Traub, N., and Kikutani, H. (1999). Mimicry of CD40 signals by epstein-barr virus LMP1 in B lymphocyte responses. Science *286*, 300–303.

Vaitaitis, G.M., Olmstead, M.H., Waid, D.M., Carter, J.R., and Wagner, D.H., Jr. (2014). A CD40-targeted peptide controls and reverses type 1 diabetes in NOD mice. Diabetologia *57*, 2366–2373.

van Kooten, C., and Banchereau, J. (2000). CD40-CD40 ligand. J. Leukoc. Biol. *67*, 2–17.

Weller, S., Faili, A., Garcia, C., Braun, M.C., Le Deist, F., De Saint Basile, G., Hermine, O., Fischer, A., Reynaud, C.-A., and Weill, J.-C. (2001). CD40-CD40L independent Ig gene hypermutation suggests a second B cell diversification pathway in humans. Proc. Natl. Acad. Sci. U S A *98*, 1166–1170.

Williams, C.J., Headd, J.J., Moriarty, N.W., Prisant, M.G., Videau, L.L., Deis, L.N., Verma, V., Keedy, D.A., Hintze, B.J., Chen, V.B., et al. (2018). MolProbity: more and better reference data for improved all-atom structure validation. Protein Sci. *27*, 293–315.

Xie, J.H., Yamniuk, A.P., Borowski, V., Kuhn, R., Susulic, V., Rex-Rabe, S., Yang, X., Zhou, X., Zhang, Y., Gillooly, K., et al. (2014). Engineering of a novel anti-CD40L domain antibody for treatment of autoimmune diseases. J. Immunol. *192*, 4083–4092.

Xue, B., Dunbrack, R.L., Williams, R.W., Dunker, A.K., and Uversky, V.N. (2010). PONDR-FIT: a meta-predictor of intrinsically disordered amino acids. Biochim. Biophys. Acta *1804*, 996–1010.

Yamniuk, A.P., Suri, A., Krystek, S.R., Tamura, J., Ramamurthy, V., Kuhn, R., Carroll, K., Fleener, C., Ryseck, R., Cheng, L., et al. (2016). Functional antagonism of human CD40 achieved by targeting a unique species-specific epitope. J. Mol. Biol. *428*, 2860–2879.

iScience, Volume *23*

Supplemental Information

Residue-Specific Message Encoding in CD40-Ligand

Aditya Yashwant Sarode, Mukesh Kumar Jha, Shubhranshu Zutshi, Soumya Kanti Ghosh, Hima Mahor, Uddipan Sarma, and Bhaskar Saha

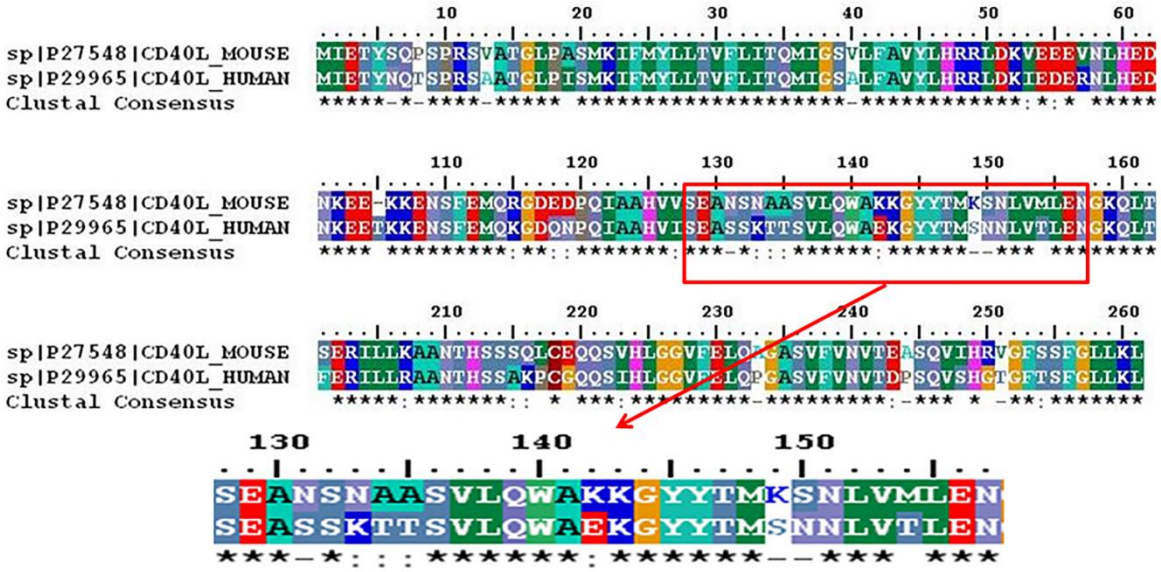

Supplementary Fig 1| Sequence alignment of human and mouse CD40L. Related to Figure 1.

Protein sequence alignment using ClustalW and matrix Blosum62 with a Gap opening penalty (GOP) of 10 and Gap extension penalty (GEP) of 0.1 was used to align human and mouse CD40L. Alignment showing residue specific color representation and (*) representation shown residue homology. (:) represents dissimilar amino acids from same group. (_) represents dissimilar amino acids form different group [group = polar, non-polar, +ve charged & -ve charged amino acids]. The residues which are important and critical in the binding of CD40 are shown in the red bracket.

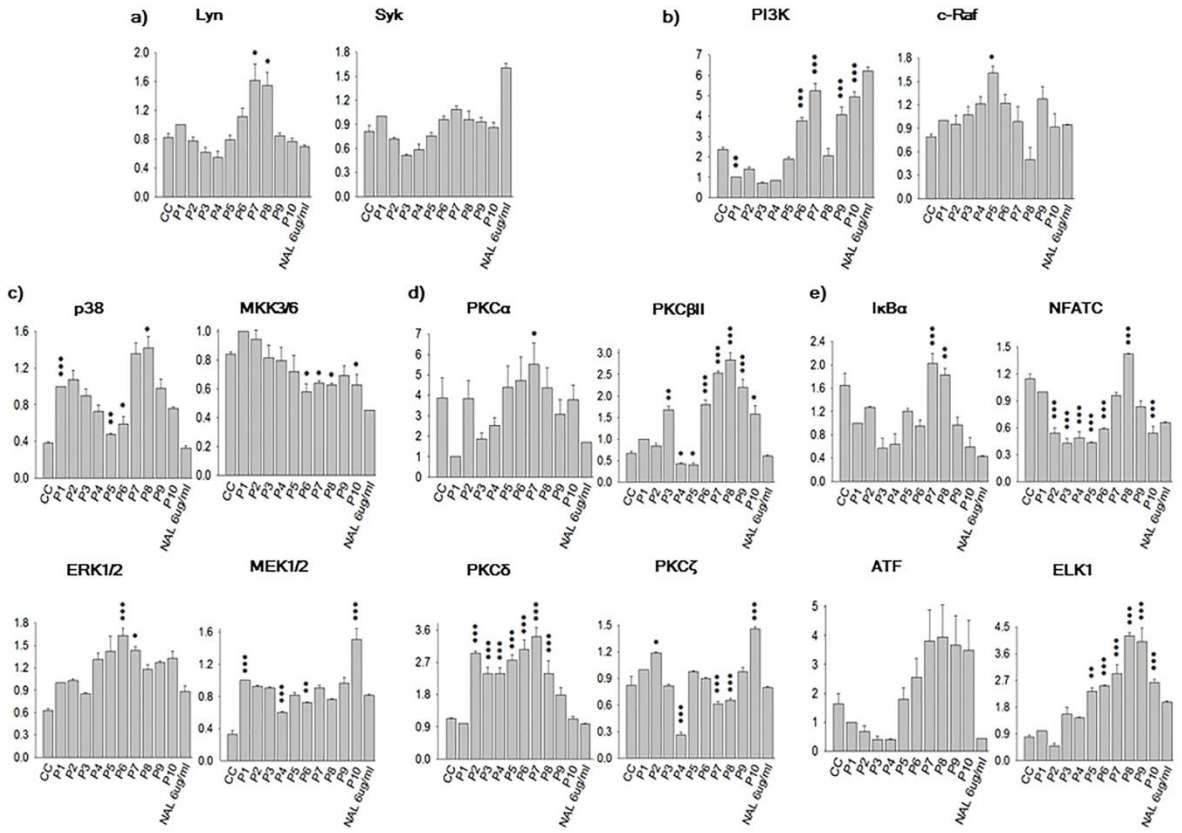

Supplementary Fig. 2| Densitometry for the activation of different signaling molecules. Related to Figure 2.

BALB/c mice were injected (i.p.) with 3% Thioglycolate media and elicited peritoneal macrophages were obtained after 5 days. These macrophages were cultured without any treatments for 36hrs. These cells were then stimulated with different mutant peptides at a concentration of 100ng/ml. αCD40 NA/LE clone 3/23 antibody (6μg/ml) was used as an experimental control. Protein lysate was prepared, and western blotting was performed to analyze the activation of different signaling intermediates. Relative activation of different signaling molecules after stimulation with mutant peptides are shown using densitometry where arbitrary values are assigned to un-stimulated cells that act as a control for calculating the relative activation in the stimulated cells. **(a)** Shows the activation of adaptor kinases Lyn & Syk, **(b)** Shows the activation of serine/ threonine kinases PI3K & c-Raf, **(c)** Shows the activation of Mitogen activated protein kinases (MAP Kinases), **(d)** Expression of PKC's. **(e)** Expression of transcription Factors using QuantityOne® software from BioRad. The data shown are mean of three independent experiments and error bars show Mean ± SEM. Statistical significance

of the differences between the means was assessed by one-way ANNOVA with Tukey's post-test, *p< 0.05, **p< 0.01, *** p≤ 0.001; n.s., not significant. For statistical significance P2 to P10 was compared to P1.

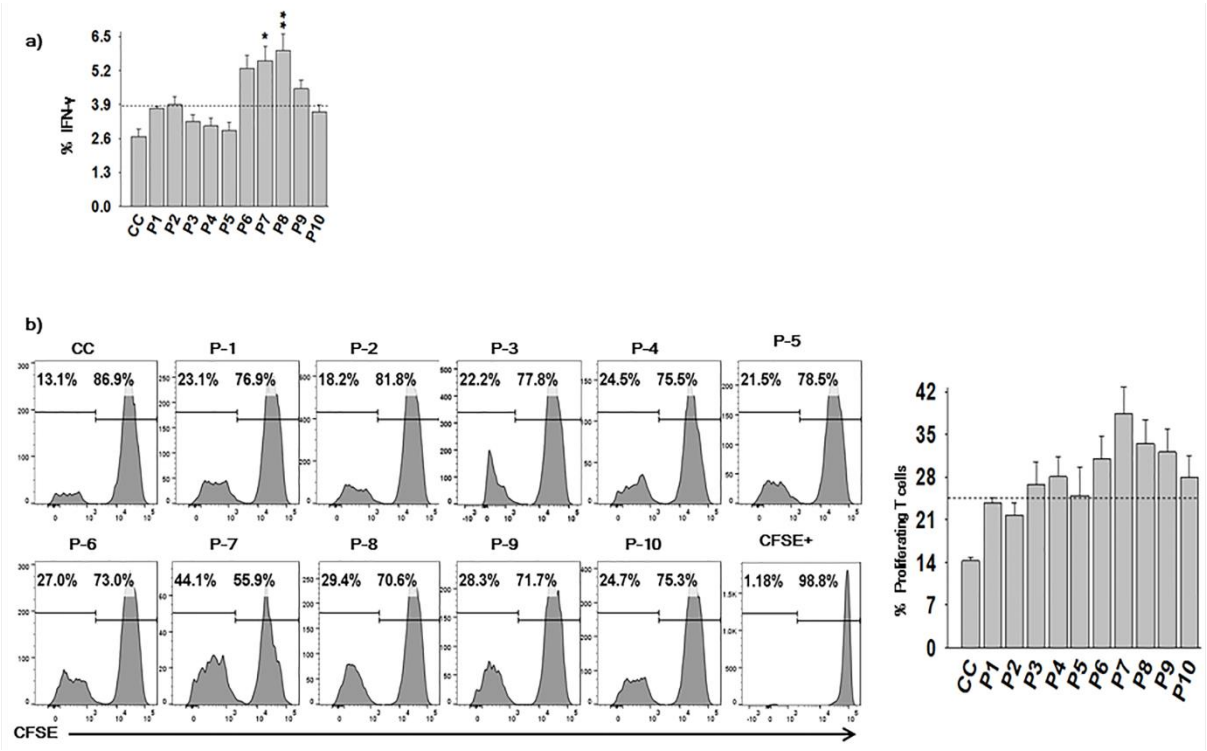

Supplementary Fig. 3| Co-culture of Macrophages-Tcells in the presence of these peptides helps in the proliferation of Tcells invitro. Related to Figure 4.

Peritoneal derive macrophages from C57BL/6 mice were cultured and rested fr 36 hrs. Following this sterile sorted CD4+CD62L-CD25- naïve Tcells from CD154-/- mice were labeled with CFSE dye and co-cultured exvivo with the 36hrs rested macrophages from C57BL/6 mice in the presence of the mutant peptides. **(a)** shows the expression of IFNγ from the CD4+ Tcells from these co-cultured system after 120 hrs. The data shown are representative for three independent experiments and error bars show Mean ± SEM. Data analysis for statistical significance was performed using one-way ANNOVA with Tukey's post-test where *p< 0.05, **p< 0.01,*** p≤ 0.001; n.s., not significant. **(b)** shows the proliferation of these CD4+ Tcells from this co-culture system after 120 hrs and the significance was drawn from three independent experiments (represented in the bar graph) where the

error bars show Mean ± SEM. Data analysis for statistical significance was performed using one-way ANNOVA with Tukey's post-test where *p< 0.05, **p< 0.01,*** p≤ 0.001; n.s., not significant. The data shown are representative for three independent experiments showing similar results.

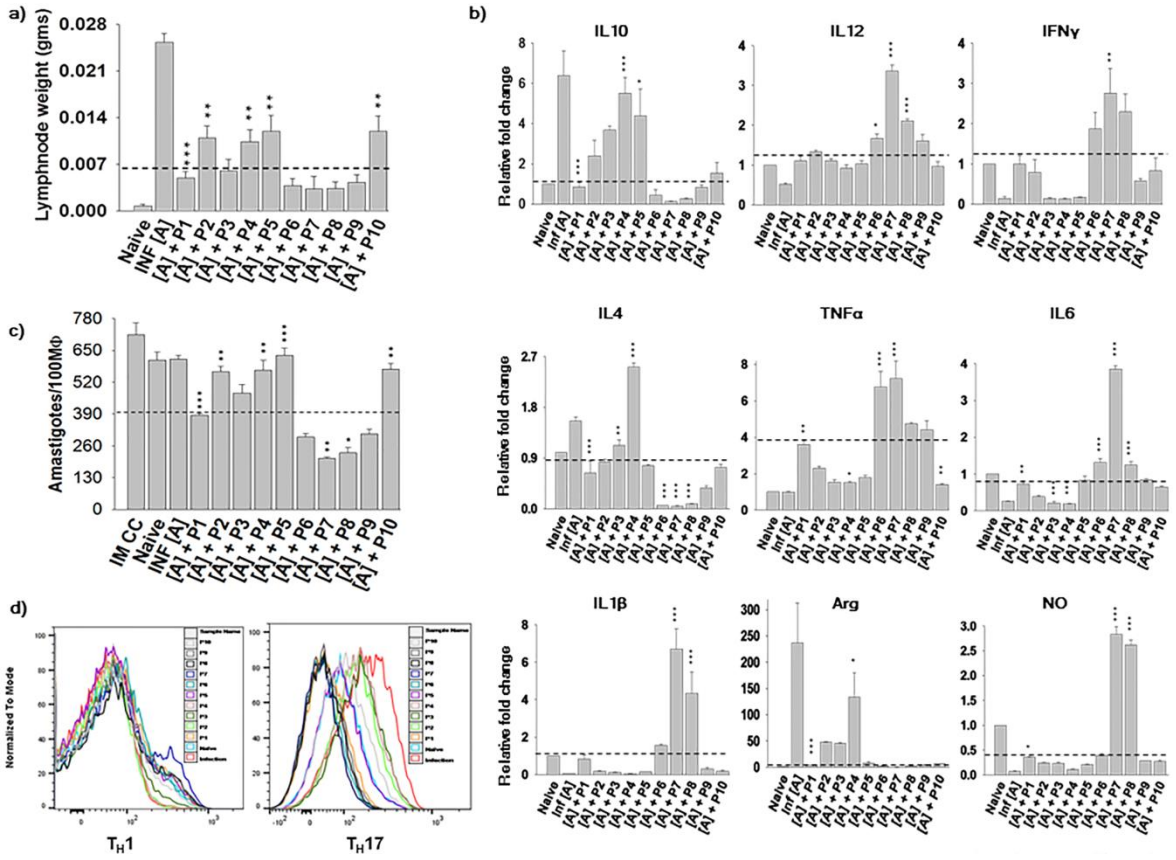

Supplementary Fig. 4| Treatment of L. major infected mice with peptide 7 and 8 reduces infection. Related to Figure 7.

Stationary phase L.major promastigotes (2 x 106) were injected (s.c.) at the hind footpad of CD40L-/- mice. Mutant peptide at a dose of 6mg/kg/mice in HBSS was administered to the mice (i.p.) mode on day 1, 3, 5 & 7 post-infection (n=5). The footpad swelling of the infected mice was monitored till 6th week (upper panel). Mice were sacrificed on 6th week and **(a)** the popliteal lymph nodes were weighed and shown as bar graph. The data shown are representative for three independent experiments and error bars show Mean ± SEM. Data analysis for statistical significance was performed using one-way ANNOVA with Tukey's post-test where *p< 0.05, **p< 0.01,*** p≤ 0.001;

n.s., not significant. **(b)** The lymphocytes from similar treated group were pooled and were subjected to quantitative Real-time PCR for the expression of different cytokines. The lymphocytes from similar treated group were pooled and were subjected to FACS analysis. C57BL/6 macrophages were infected with stationary phase L. major promastigotes at a macrophage: parasite ratio of 1:10 for 8hrs. Unbound parasites were washed and macrophages were rested for 48hrs. Lymphocytes obtained from the peptide treated mice were co-cultured with these L. major-infected macrophages along with CSA (10 μg/ml) for 72hrs. **(c)** Shows the number of amistigotes/100 macrophages in this co-culture system. The data shown are representative for three independent experiments and error bars show Mean ± SEM. Data analysis for statistical significance was performed using one-way ANNOVA with Tukey's post-test where *$p< 0.05$, **$p< 0.01$,*** $p\leq 0.001$; n.s., not significant.The lymphocytes from similar treated group were pooled and were subjected for FACS analysis. **(d)** Shows the expression of t-bet expressing Th1 & RoR-γt expressing Th17 gated on CD4+CD44+CD62L- T-cell subsets. The figure represents the overlay of (MFI) normalized to mode in the gated population. The data shown are representative for three independent experiments showing similar results.

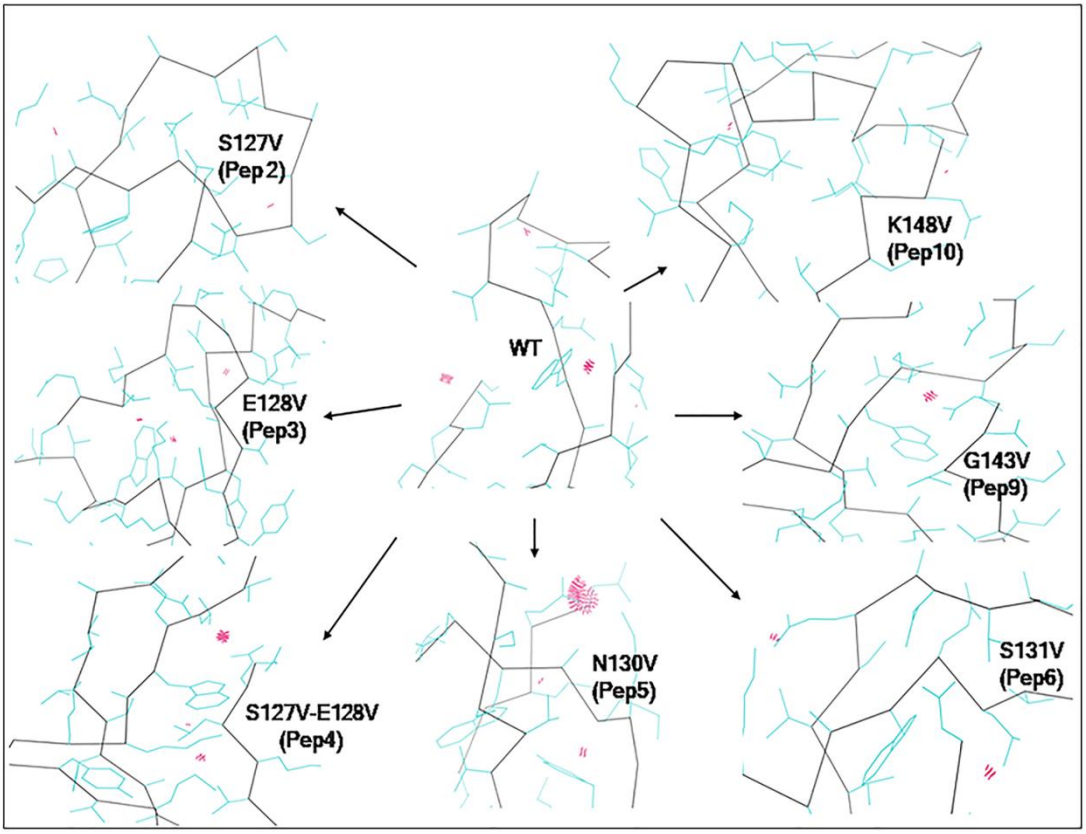

Supplementary Fig. 5| Clashes within the structures. Related to Figure 8.

I-Tasser predicted structures of CD40L 41mers (Wild type and mutated) are analysed by Molprobity and the kineimage are visualized by KiNG software showing clashes in the structures of Pep1, Pep2, Pep3, Pep4, Pep5, Pep6, Pep9 and Pep10. Hot Pink: Serious Clash Overlap ≥ 0.4Å. All the structures have variable residues introducing clash overlaps. No clash overlaps were visualized in Pep7 and Pep8.

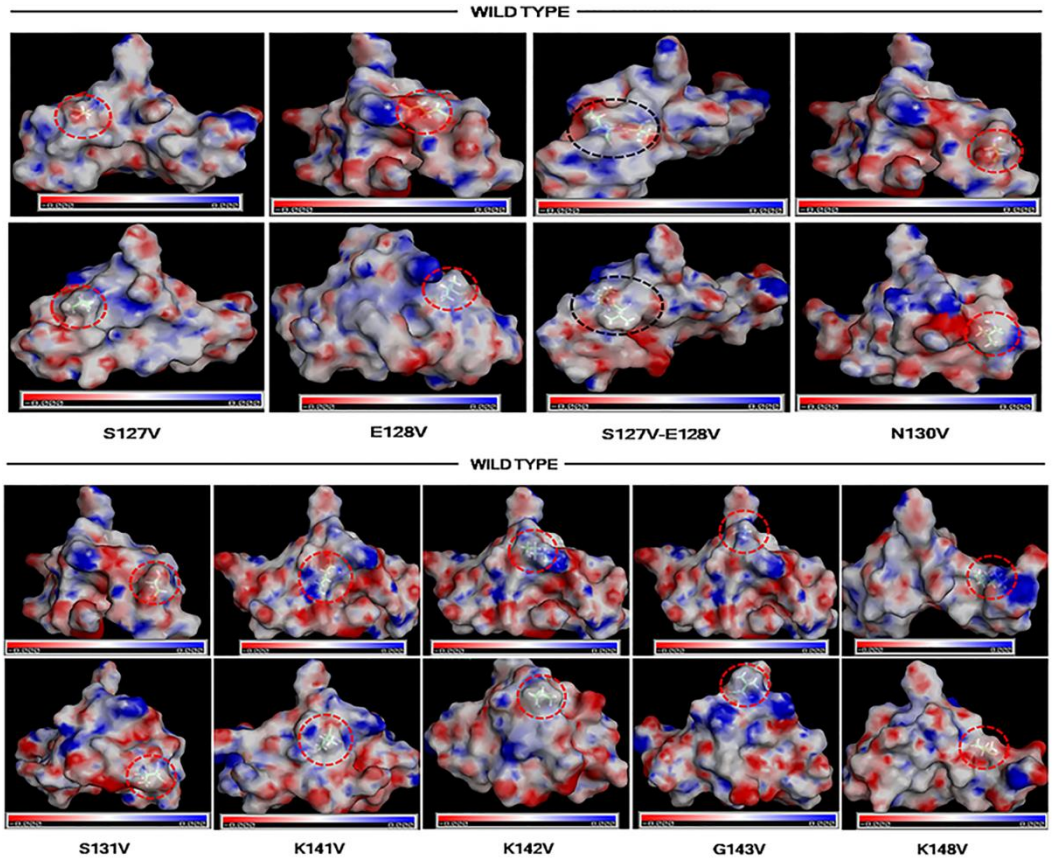

Supplementary Fig. 6| Electrostatic Surface Potential comparison between wild type and mutated peptides. Related to Figure 8.

Localized variation in electrostatic surface charge is identified after substitution to Valine. All mutations imparted difference in position specific surface potential except, S124V-E126V (Pep4). The Pep2 (S127V), Pep3 (E128V) and Pep6 (S131V) mutations induces electrostatic surface potential from negative to positive, whereas the Pep7 (K141V) and Pep10 (K148V) mutations induces from negative surface potential compared to positive charge surface of wild type peptide.

Materials

Reagents

Antibodies against pPI3K (4221), pcRaf (9427), pLyn (2731), pSyk (2711), pPKCα (9375), pPKCβII (9371), pPKCδ (9376), pPKCζ (9378), pp38 (9276), pMKK3/6 (9231), pMEK1/2 (9121), pATF2 (9221), pELK1 (9181), Lyn (2732), Syk (2712) were procured form **Cell Signaling Technology**. Antibodies against pERK1/2 (Sc-7383), p38 (Sc-7972), ATF2 (Sc-187), ELK1 (Sc-22804), pNFAT (Sc-32978), NFAT (Sc-7294), pIκBα (Sc-8404), ERK1/2 (Sc-154), MKK3/6 (Sc-13069), MEK1/2 (Sc-436), PKCα (Sc-208), PKCβII (Sc-13149), PKCδ (Sc-8402), PKCζ (Sc-17781), IκBα (Sc-371), PI3K (Sc-293172), cRaf (Sc-28772), HMGCoA (Sc-SC-27578) and Filipin (Sc-205323) and Ultracruz Mounting Medium (Sc-24941) were procured from **Scantacruz**. Antibodies PerCP-eFluor™710 anti Arginase (46-3697-82), PE anti iNOS (12-5920-82), PE anti RoRγ (12-6981-82) were from ebioscience. Antibody against Ceramide Synthase (C8104-5OTST), Tri™Reagent (T9424), Streptavidin POD Conjugate (11089153001), Griess reagent (modified) (G4410) were from **Sigma / Roche**. Antibodies FITC anti CD4 (557307), FITC anti Annexin V (51-65874X), 7-AAD (559925), PE anti BATF (564503), Alexa Fluor® 647 anti Blimp-1, Pacific blue anti CD4 (558107), APC-Cy7 anti CD25 (557658), PE-Cy7 anti GITR (558140), Alex®647 anti Foxp3 (563486), PE anti IL-10 (554467), Per-CP™5.5 anti CD44 (560570), APC-Cy ™7 anti CD62L (560514), FITC anti CD19 (553785), APC anti IgD (560868), Purified anti IL-4 (554387), Biotin anti IL-4 (554390), Purified anti IL-6 (554400), Biotin anti IL-6 (554402), Purified anti IL-10 (551215), Biotin anti IL-10 (554423), Purified anti IL-12 (551219), Biotin anti-mouse IL-12 (554476), Purified anti TGF-β1 (555052), Biotin anti TGF-β1 (555053), Purified anti TNFα (557516), Biotin anti TNFα (557432), Purified anti IFNγ (551216), Biotin anti IFNγ (554410), TMB Substrate Reagent Set (555214) was from **BD Pharmingen**. Antibodies PE anti CD274 (124307), PECy7 anti CD11b (552850), Per-CP Cy5.5 anti CD127 (121114), APC anti IL-17A (506916) were from **Biolegend**. Clarity Max Western ECL Substrate (1705062) from **BioRad**. CFSE dye (C34554) was from Invitrogen. RPMI 1640 (12633012), PenStrep (12430062) was from **Gibco™ Invitrogen**.

Methods

Mice and macrophages isolation:

BALB/c, C57BL/6 and CD40L$^{-/-}$ mice originally obtained from Jackson Laboratories, USA, and was bred in the institute's experimental animal facility. For all the experiments 6-8 weeks old mice were used. Standard laboratory conditions and settings were used to maintain all the animals. Macrophages, elicited by injecting 2ml of 3% thioglycolate (i.p.) in mice were isolated after 5 days and cultured in advanced RPMI-1640 (reduced serum medium; catalogue #12633; GIBCO, Grand Island, NY) supplemented with 6% fetal calf serum, penicillin-streptomycin and 2-mercaptoethanol followed by resting for 36hrs.

Parasite culture and in vitro infection:

Leishmania major promastigotes (5ASKH) were maintained in RPMI-1640 with 10% fetal calf serum in vitro. In order to maintain the virulence of the parasites the parasites were injected subcutaneously into the left hind foot-pad of BALB/c mice. Cultured macrophages were infected with parasites at a ratio of [1:10] Macrophage: Parasite for 8 hrs at 33ºC in 5% CO_2 incubator followed by washing of extracellular parasite. All experiments related to parasite infection were carried out with either 48 or 72hrs infected macrophages.

Peptide Synthesis:

Peptides were custom synthesized commercially from Genscript®USA. The peptides were >98% pure and were TFA removed and the solubility was checked using their in-house solubility check. The peptides were further checked for QC. The peptides were dissolved according to the manufacturer's protocol. More details of the procedure can be obtained from *https://www.genscript.com/peptide_tech.html*

RNA isolation and Semi quantitative and Real-time PCR:

Total RNA was isolated from the uninfected or infected cells using TRI reagentTM (Sigma) according to manufacturer's instructions. For cDNA synthesis, 2µg of total RNA from each sample was incubated with random primer and heat inactivated at 65ºC for 5 min. Heat inactivated sample was incubated with 0.1 mM DTT, 500µM dNTPs, 40U RNase inhibitor, and 1µl of MMLV-reverse transcriptase at 37°C for 1 h followed by incubation at 65ºC for 10 min.

Immunoblotting:

After the respective treatment cells were washed with chilled PBS and then lysed in lysis buffer (20mM Tris-HCl pH 7.5, 150mM NaCl, 1mM EGTA, 1mM EDTA, 10% glycerol, 1% NP40, protease inhibitor cocktail from Roche and phosphatase inhibitor from Pierce). Western bolts were performed on these lysed samples. Samples were loaded on gel for western blot analysis using 4x loading dye and the images were acquired on Amersham Imager 600 imagers. The densitometry was performed using Quantity One software from BioRad. The densitometry values for each signaling molecule were normalized using the total of the same. These were values were normalized with the wild type peptide stimulated values. Heat map was generated in R using lattice graphics library package and level plot () functions.

Parasite load assay:

$5X10^4$ peritoneal macrophages were plated in 8 well chamber slides (Co star). Cells were infected with L. *major* parasite at a ratio of [1:10] Macrophage: Parasite for 8 hrs followed by resting for 48hrs. The treatments with peptides were given for 72 hrs. After 72hrs infection, cells were washed and stained with Giemsa as described earlier and the supernatant was subjected to NO estimation, using Grease reagent supplied from SigmaAdrich and the OD was taken at 450nm and values were plotted.

Confocal microscopy:

Thioglycolate-elicited BALB/c-derived peritoneal macrophages were seeded at a density of 2 X 10^6 cells on 22 X 22 mm cover slip placed in a 6 well plate. Cells were infected with L. *major*

promastigotes parasites which were labelled with CFSE dye. In brief parasites were washed 3 times with plain media followed by staining of the parasite with CFSE dye for 20min at 37 in dark. The staining was stopped using 10% FCS containing media followed by 3 washes. The parasites were counted and were used to infect the mice macrophages as described above. For immunofluorescence staining, cells were washed thrice with cold PBS, treated with pre-chilled methanol (2 min on ice), washed with ice cold PBS twice and were stained with Hoechst 33342 (0.1mM; r.t., 30 min., dark). Washed thrice with PBS, cells were mounted and Images were acquired under a Leica SPII microscope under blue and green channels.

In vivo parasite infection and peptide treatment:

C57BL/6 and CD40L$^{-/-}$ mice were infected subcutaneously on left hind footpad with 2x10^6 L. *major* parasites on day 0. Mutant peptide at a dose of 6mg/kg/mice in HBSS was administered to the mice (i.p.) mode on day 1, 3, 5 & 7 post-infection. The swelling in the footpad were measured using vernier caliper and the readings were subtracted from the reading of the uninfected footpad in order to calculate the footpad thickness. Six weeks post infection, mice were sacrificed and lymph nodes were collected and parasite load in the draining lymph node was assessed as described earlier and the lymphocytes were used for recall response, co-culture and FACS analysis.

Staining of cells for FACS:

Cells were stained on surface or intracellular as described by Martin et al.(Martin et al., 2010) Macrophages were harvested using cell scraper and washed using FACS buffer containing 2% FCS. Cells were blocked using 10% FCS for 30 min at 4 ºC followed by washing 2 times. For surface labeling cells were stained using the preferred antibody according to the manufacturers recommended titer for 45 mins at 4ºC in dark. The cells were further washed 2 times followed by either intracellular staining or re-suspending them in 1%PFA containing solution. For intracellular staining Intracellular Cytokine Staining kit (BD Pharmingen) was used, following the manufacturer's protocol.

Lymph node from the 6 week *L.major* infected mice were crushed and washed twice with 1X PBS, cells were centrifuged at 1200 rpm (Eppendorf 5810R centrifuge). Cells were resuspended and

stimulated with PMA (20 ng/ml)-ionomycin (1 µg/ml) for 4hrs followed by GolgiPlug (1mg/ml) for 2 hrs. Cells were then washed, followed by blocking in 10% FCS (30 min at 4ºC). This was followed by staining with the surface antibodies for 45min and the cells were then washed twice. Intracellular staining was performed as per above procedure. Cells were washed twice before acquisition on FACS CantoII machine with proper controls and fluorescent compensations. The data was analyzed on FlowJo software.

Cytokine ELISA:

Culture supernatants are sampled for Sandwich ELISA to detect cytokine profile investigation using BD Pharmingen manual. Plates are coated with 50 ul of anti-cytokine mAbs in Phosphate buffer (PH 7.4) for 12hrs at 4ºC temperature. Plates are washed twice with wash buffer (PBS, 0.05% Tween 20) and to avoid non specific binding the wells are blocked with 100µl blocking buffer (PBS and 1% BSA) for 4 hours and again washed twice with washing buffer. After wash, 100µl of murine recombinant cytokine standard or supernatant sample is added and kept for 18 hours at 4ºC. Twice 100µl wash buffer wash is done and followed by adding of 100µl of Biotin-labelled anti-cytokine mAbs for 1 hour at 4ºC. After two time wash with wash buffer, 100µl peroxide-conjugated streptavidin is added and incubated in room temperature for 45 mins. To the ELISA plate another two times wash is given and each well is added with 100µl tetramethylbenzidine substrate (BD Pharmingen). After an incubation period of 10-20 minutes at room temperature stopping solution (1N Sulphuric acid in double dH2O) is added and the absorbance at 450 is measured by automated micro plate absorbance reader.

Real-time PCR:

Real-time PCR is performed on peritoneal macrophages and splenic T cells, which are lysed using TRIzol reagent (Sigma-Aldrich, St. Louis,MO). Reverse transcrptase (Invitrogen, Carlsbad, CA) and random primers are used to prepare cDNA and the Real time RT-PCR is performed using SYBER green enzyme master mix. Step-OnePlus Real time PCR system (Applied Biosystems) is used to perform PCR with 10µl reaction volume consisting of 4.6µl of cDNA sample (diluted in nuclease-free

water) and 5.4µl volume of SYBER green enzyme and primer master mix. The mRNA expression is normalized to the median expression of housekeeping gene (GAPDH).

Structure and disorder prediction:

The structure prediction of the whole and 41mer residue wild type and other mutated sequence of ligand are conducted with I-Tasser server. The CD40 structure is too predicted with I-Tasser server due to lack of complete CD40 structure in protein data bank. Structural disorder study of wild type and each mutated (whole) structure is studied by DisEMBL, GlobPlot and PONDR. The prediction methods are different and discussed in (papers). Structural verification of the 41mer sequences of wild type and mutated CD40 ligand is performed using MolProbity. MolProbity is also used to prepare kinemage format files of each PDB files. KiNG program analyzed and detailed the atoms with clash and contacts in the kinemage files.

Protein – Protein docking:

In silico CD40 receptor is docked with wild type and mutated CD40Ligands using HADDOCK webserver. CPROT is used to list the active and passive participating residues of receptor and ligands to be filled while submitting job to HADDOCK webserver. No inputs on specific site for contacts are made to avoid biased submission.

Data analysis and heat map generation:

Each replicate of in-vivo data was normalized to the expression level when subjected to the wild type ligand (P1; WT control). The median of the 3 replicates is calculated and the data is log2 transformed to better visualize fold changes upon residue replacement. Values obtained in the range 0.5-2 fold (of WT control) are considered in the range of experimental noise and were reassigned the value of 1 (or 0 in log2 scale). The data thus processed is plotted as a heatmap shown in Fig 6.

Statistical analysis:

All the in vivo experiments were performed on three different times with a minimum of 5 mice per group. The results are described as Mean ± S.E.M. The significant of difference between the means was determined by one-way ANNOVA with Tukey's post-test where *$p < 0.05$, **$p < 0.01$, *** $p \leq 0.001$; n.s., not significant. For testing the statistical significance, P1 (wild type) was compared to the cell control whereas P2 to P10 was compared to P1 (wild type)

References:

MARTIN, S., AGARWAL, R., MURUGAIYAN, G. & SAHA, B. 2010. CD40 Expression Levels Modulate Regulatory T Cells in Leishmania donovani Infection. The Journal of Immunology, 185, 551-559